MECHANISMS AND IMPLICATIONS OF CHANGES IN THE TIMING OF OCEAN FREEZE-UP

By

Rebecca J. Rolph, M.Sc.

A Dissertation Submitted in Partial Fulfillment of the Requirements

for the Degree of

Doctor of Philosophy

in

Geophysics

University of Alaska Fairbanks

August 2018

APPROVED:

Dr. Andrew Mahoney, Committee Chair
Dr. John Walsh, Committee Member
Dr. Hajo Eicken, Committee Member
Dr. Peter Winsor, Committee Member
Dr. Philip Loring, Committee Member
Dr. Sarah Fowell, Chair
Department of Geosciences
Dr. Anupma Prakash, Dean
College of Natural Science and Mathematics
Dr. Michael Castellini, *Dean of the Graduate School*

Table of Contents

Page

Abstract

The shift to an Arctic seasonal sea ice cover in recent years motivates a deeper understanding of freeze-up processes and implications of a lengthened open water season. As the sea ice boundary between the Arctic ocean and atmosphere covers a smaller area, the effects of enhanced wind mixing become more pronounced. Winds are important for ocean circulation and heat exchange. Ultimately, they can influence when freeze-up can occur, or can break up new ice as it forms. The chapters of this thesis are motivated by the substantial social and geophysical consequences of a lengthening open water season and linked through discussion of what controls freeze-up timing.

Implications of a declining sea ice cover as it pertains to the three Arctic Alaska coastal communities of Kotzebue, Shishmaref, and Utqiaġvik are explored in depth. Indices of locally-relevant metrics are developed by using physical climate-related thresholds found by other studies to impact Alaska communities and coastal erosion rates. This allows for a large-scale climate dataset to be used to define a timeseries of these indices for each community. We found a marked increase in the number of false freeze-ups and break-ups, the number of days too windy to hunt via subsistence boat, and in Utqiaġvik, an approximate tripling of erosion-capable wind events from 1979-2014.

The WRF-downscaled ERA-Interim dataset (ERA-Interim for sea ice) was also used in the analysis of all chapters. The cumulative wind energy input into the upper ocean was calculated for the Chukchi, southern Beaufort, and northeast Bering Seas at time periods up to three months prior to freeze-up, and then correlated with the timing of freeze-up. We have found that increased wind energy input into the upper ocean 2-3 months prior to freeze-up is positively and most strongly correlated with the date of freeze-up in the Chukchi Sea. Analysis of wind climatology shows winds are increasing in the period prior to freeze-up as a delayed freeze-up moves into the fall storm season. A negative correlation is found in the Bering Sea over shorter timescales, suggesting that storms promote the arrival of sea ice there. Case studies are evaluated for the Chukchi Sea and Bering Sea, to illustrate mechanisms at play that cause the positive and negative correlations in these seas, respectively. Ice advection and high winds from northerly directions are shown to hasten the timing of freeze-up in the Bering Sea. In the Chukchi Sea, higher winds from the dominant northeasterly direction promote upwelling of warm and salty water up onto the shelf, which suggests a mechanism for why high winds are associated with a delayed freeze-up there.

We next examine the effect of winds on freeze-up timing by using a 1-D vertical column model of the mixed layer. The model is initialized using temperature and salinity profiles obtained from a freeze-up buoy deployed in 2015 in the north-east part of the Chukchi Sea. The meteorological forcing used to drive the model experiments comes from a WRF-downscaled ERA-Interim Reanalysis dataset. Our results show that vertical wind-driven mixing leads to enhanced heat loss. In light of the previously found positive correlation between wind energy input and freeze-up timing, the mixing model results suggest horizontal advection not captured by the 1-D column model can dominate wind-driven vertical mixing to promote freeze-up.

List of Figures

Page

List of Tables

Page

Acknowledgements

This work would not have been possible without the support from my committee, especially my advisor Andy Mahoney, and John Walsh. Andy has been very supportive, giving valuable advice which I will try my best to carry forward as I begin to start my academic career. He gave me the chance to start this PhD, and I have learned a lot because of him. John Walsh somehow always found the time to give constructive, detailed, and thoughtful feedback, and I am very much looking forward to collaborating with him during future projects. Hajo Eicken has asked great questions about my research, which led to analysis I feel has significantly contributed to the project. Phil Loring was an asset to have on my committee in the sense his participation guided a practical aspect of my thesis so it is relevant to members of Arctic communities. Discussions with Peter Winsor helped me be prepared for what to expect during the scientific process. Andy Aschwanden and the Alaska Region Supercomputing Center helped provide technical support for which I am thankful. My funding sources were from the ArcSEES NSF award 1263853 and the Center for Global Change (CGC) Student research competition, for which I am also thankful.

I want to thank my supportive friends, in no particular order, Devin McDowell, Erica Blake, Thilo Klenz, Anika Pinzer, Jane Lanford, Rick Lader, Erica Burr, David Fee, Taryn Lopez, Katie Galloway, Nora Vassileva, Kim Alizadeh, Caitlin Van Ort, Charlie Parr, Nick Janssen, Bob Torgerson, Jon Hutchinson. The West Ridge Runners, who have been a consistent and irreplaceable part of my life in Fairbanks. Matthias Fuchs has always been there for me when I need him, I didn't think it was possible for someone to be so supportive. I would also like to thank my mom, who has taught me what is important. Drew Harrington and the ultra running community in Fairbanks have brightened the way for many future opportunities I before did not know existed.

Chapter 1

Introduction

1.1 Background and Motivation

A reduction in the extent of Arctic sea ice in recent years, illustrated by satellite products, is one of the clearest and therefore most common indicators used to show that our climate is rapidly changing. Sea ice is an important part of the changing climate and has shown accelerated rates of change compared to many other components of the climate system. Due to its importance in the climate system as a whole, in conjunction with an accelerated decline in the extent of sea ice cover (Comiso *et al.*, 2008), it is not surprising that sea ice is frequently referenced in the public media. Climate change has far reaching consequences outside of the Arctic regions. Mid-latitude weather (Cohen *et al.*, 2014; Francis and Vavrus, 2012), fast increases in global temperature, changes in animal migration (Hauser *et al.*, 2017), and easier navigation of trans-Arctic commerical ocean routes (Smith and Stephenson, 2013) have all been suggested to be caused at least in part by a receding ice cover.

The length of the open water season is influenced by when freeze-up occurs. The mechanisms and impacts of the freeze-up season itself are therefore important, but also at the moment not as well invesigated as break-up processes (Perovich *et al.* (2008); Kohout *et al.* (2014); Mahoney *et al.* (2007) and Belchansky *et al.* (2004)). In recent years, the geophysical scientific community has begun to understand the great value of community observations from indigeneous people, whose subsistence lifestyles are heavily impacted by the timing of when sea ice cover develops (Gearheard *et al.*, 2017). Now, the processes of freeze-up are beginning to receive increased attention (Smith *et al.* (2018), Stroeve *et al.* (2016)). This is an important step to further understand not only how the sea ice cover is changing, but what mechanisms are involved such that future projections of our climate can be improved.

1.2 Implications of a lengthened open water season on Alaska communities

1.2.1 Coastal erosion

As Arctic sea ice cover declines, coastal erosion is becoming more of an issue because sea ice acts to dampen wave action applied to the coastline. Erosion on Alaska's Beaufort Sea coast has increased roughly three times from 6.8 to 19 m per year since 1955, when the open water season has increased about 2 times since 1979 (Barnhart *et al.*, 2014). This thesis examines the three different communities of Utqiaġvik, Kotzebue, and Shishmaref which also differ in their geomorphological make-up and so their vulnerability to coastal erosion. Utqiaġvik, on the northeastern coast of the Chukchi Sea, consists of coastal bluffs which are composed of ice and organic contents (Brown *et al.*, 2003). These coastal bluffs erode at rapid rates via so-called notch erosion, which is when warmer water cuts away at the base of the cliff, and eventually develops a notch too deep for the cliff to remain stable, so it collapses into the ocean and the sediment is carried away. This type of erosion is accelerated by late summer and fall storms generating winds from the southwest (Brown *et al.*, 2003), which raise water levels along the coastline. In the northern Chukchi Sea, ice shove events alter the profile of gravel beaches, much more than in the southern Chukchi Sea where the shelf is shallow and offshore gradient is smaller. Storms can produce large storm

surges along the Seward Peninsula coast, with high waves at Shishmaref and raised sea levels at Kotzebue (Mason *et al.*, 1997). The predominant sediment in the southern Chukchi Sea is medium to fine sand, silt, and clay (Mason *et al.*, 1997), which are more readily transported and deposited elsewhere to aggrade/erode barrier islands.

1.3 Definition of freeze-up and the open water season

Indigenous communities use the sea ice as a platform for hunting and fishing, and over-ice travel by snowmachine or street vehicles. They hunt animals that also rely on the sea ice, who use it as a platform for feeding, breeding, raising young, and resting, such as bearded seals and walrus (Kovacs *et al.*, 2011). In contrast, commericial activities view sea ice as a hazard, since it poses a threat to barge and vessel travel (Smith and Stephenson, 2013). The transition period between open water and sea ice cover is a time period where neither water or over-ice travel is viable due to concerns of safety in terms of collisions with drifting ice floes or the possibility of breaking through thin sea ice.

In terms of identifying when and where sea ice or open water use is viable for transportation, it is important to develop methods which can be used on a large spatial domain. The same methods should be applicable across communities or even across heavily-trafficked vessel routes. A sea ice concentration threshold, or a minimum percentage of sea ice cover over a particular area of the ocean, is commonly used as a metric for defining whether or not an area is ice-covered. But, the threshold of sea ice concentration that determines ice cover versus open water may be debatable, depending on who is asked, or what the purposes of the study are. For example, the timing of freeze-up as given by a large-scale definition may not match a local observation of freeze-up timing along the coastline. Another definition of freeze-up could be when the water reaches freezing temperature. From a scientific or geophysical perspective, 15% sea ice cover is a common threshold used for defining the sea ice edge (Cavalieri *et al.*, 1999; Francis *et al.*, 2009; Stroeve *et al.*, 2008). Work by Johnson and Eicken (2016) compared the freeze-up and break-up dates determined by an algorithm they introduce which uses passive microwave satellite data, with dates community members in Utqiaġvik considered as freeze-up and break-up.

The general annual cycle of sea ice concentration at a point along the coastline which experiences a freeze-up and break-up each year begins with sea ice cover during winter, a subsequent melt season, an open water season, followed by a freeze-up transition back into the ice covered season. When examining freeze-up timing, sometimes it is problematic to account for the fact the sea ice can freeze-up or break out multiple times before finally transitioning to open water or sea ice cover for the season. This led to some discrepancies in the passive microwave algorithm for freeze-up detection and local community observations for the years 2006 and 2007 in Johnson and Eicken (2016). In this thesis, we have defined these events as 'false freeze-ups' and 'false break-ups'. In Chapter 2 we examine the increasing trends in the number of false freeze-ups and break-ups in recent years.

Once we identified an appropriate method for defining freeze-up (here we have chosen a pre-

scribed threshold of satellite-obtained sea ice concentration), we then begin to ask questions about the geophysical mechanisms that cause freeze-up. After understanding the mechanisms, it will help in freeze-up prediction. With the help of climate models, understanding freeze-up mechanisms on a timescale of storms can aid in determining if freeze-up should be expected to be hastened or delayed on a seasonal scale.

1.4 The importance of wind-driven mixing of the upper ocean and influence on freeze-up timing

Storms can deepen the mixed layer substantially as they pass (Rainville *et al.*, 2011). This increases the amount of heat in the mixed upper ocean which needs to be lost before freezing temperature can be reached. Given the same net heat flux, the process of wind-driven mixing in this context will result in a longer time before freezing temperature is reached, because more heat must be lost. However, increased wind speeds also increase turbulent heat loss out of the ocean. For these reasons, and those discussed in more detail later in the thesis, any changes in the amount of wind energy input prior to freeze-up can influence the timing of freeze-up.

Fall tends to be a time of heightened wind speeds and increased numbers of storms. Figure 3.3a gives the week number of the highest daily-averaged wind speeds for the Chukchi, southern Beaufort, and eastern Bering Seas. As freeze-up shifts later in the year, it is also shifting to occurring more into the fall storm season. Thus, we should expect an increase in wind speeds in the months prior to the timing of freeze-up. Wind energy transfer from the atmosphere to the ocean should also therefore be expected to increase in the months prior to freeze-up, along with associated wind-driven upper ocean mixing. It is important to understand how these trends are evolving, because increases in wind speeds and fetch (distance of open water) also increase the significant height of wind-waves (Taylor and Yelland, 2001). Wind waves are considered a significant hazard for Arctic shipping (Aksenov *et al.*, 2017), threat to coastal infrastructure, and have been observed to increase shoreline erosion (Overeem *et al.*, 2011). For these reasons, an increase in wind wave action during the fall freeze-up season is likely to have negative consequences. Understanding how increases in upper ocean wind energy input are changing in the months prior to freeze-up, and at the same time elucidating how this change in energy input influences freeze-up timing, is therefore valuable to coastal stakeholders.

The impact of wind and storm-driven mixing on the upper Arctic Ocean has been previously examined (e.g. Toole *et al.* (2010) and Long and Perrie (2012)), but these studies examine waters where sea ice is already present. What is lacking is how the timing of enhanced wind-driven mixing can influence the timing of freeze-up. Specifically, what is lacking is how mechanical mixing and turbulent surface heat fluxes induced by winds impact the heat content of the upper ocean prior to freeze-up. Long and Perrie (2012) found that the temperature of the sea surface can cool as much as 2°C if there is cool water being mixed up from below by storms towards the warmer surface. However, this may have been an observed anomaly for this location, because whether or not the sea surface is warmed or cooled by mechanical mixing from a storm depends

on the initial temperature profile before the storm passes. For example, in contrast to the results of Long and Perrie (2012) (but following along the same lines in terms of mechanism), Yang *et al.* (2004) found a warming of sea surface temperature after a storm penetrated the halocline (depth of sharp salinity and density gradient) and brought warm subsurface water upwards.

These contrasting results lead to the question of: 'What is the overall, mean impact of a stormy season in the months prior to freeze-up?' In other words, given that there have been differences in individual storms on the temperature of the sea surface, is there an overarching mechanism which can be found that would help to predict whether or not freeze-up should be delayed or hastened, given a calm or windy few months prior to freeze-up? How much would a few individual large storms matter, immediately prior to freeze-up, as opposed to an overall windier season in the months prior? We investigate these questions in the subsequent chapters of this thesis.

The primary research questions addressed in the subsequent chapters are:

1. How are coastal communities affected by changes in the length of the open water season and how can we assess these impacts using large scale datasets?

2. What are the implications for increased wind stress over open water due to delayed freeze-up?

3. Do storms promote or delay the freeze-up process?

4. What role does wind mixing play in preconditioning the upper ocean for freeze-up?

1.5 Thesis outline

Chapter 2 is a study of how changes in the open water season length and seasonal transition between open water and ice impacts Alaska coastal communities and provides analysis to answer Question 1 above. Thresholds of geophysical variables (e.g. wind speed, wind direction, and sea ice concentration) are used to develop locally-relevant indices from large scale datasets and community observations. The thresholds used have been selected because they have been shown from other studies to impact Alaska community ways of life. For example, a wind speed threshold was used to quantify trends in the number of days deemed 'too windy' to hunt via boat in open water (Ashjian *et al.*, 2010). As a delayed freeze-up moves into the fall storm season, there is a need to evaluate recent and future trends in winds over open water. Coastal erosion is also impacted by high wind speed, but also direction, since along to onshore wind direction causes water set-up along the coastline, accelerating transport of sediment (Overeem *et al.*, 2011). In Chapter 2 we also quantify the number of high wind events which occur in the wind directions most conducive to erosion at three Alaska coastal communities of Utqiaġvik, Kotzebue, and Shishmaref.

Chapter 3 aims to answer Questions 2 and 3 above and begins to refine the scope of this thesis. Chapter 3 evaluates multi-decadal trends in cumulative wind energy input into the upper ocean and wind speeds prior to freeze-up (specifically the Chukchi and southern Beaufort seas). These are important to understand given how wind plays a role in the timing of freeze-up (Section

1.4). Additionally, information about storminess prior to freeze-up is important for Arctic coastal communities. This is because before sea ice cover exists to dampen storm-driven wave action, problems relating to erosion and travel are amplified. Chapter 3 also evaluates correlation values between the timing of freeze-up and cumulative wind energy input into the ocean in at various periods before freeze-up.

Further narrowing the scope of the thesis, Chapter 4 delves deeper into the physical mechanisms of freeze-up using a 1-D vertical ocean column model (Price *et al.*, 1986). This aims to answer Question 4 above. We test the sensitivity of freeze-up timing of the surface ocean with different properties (temperature, salinity profiles) and changes in meteorological forcing of high, average, and low wind seasons. Temperature and salinity profiles (stratifications) come from an ice detection buoy deployed in 2015 in the north east part of the Chukchi Sea (Alaska Ocean Observing System, 2018).

A concluding chapter (Chapter 5) summarizes the main results found across all chapters. It also condenses the results into a context of how this thesis has contributed to understanding the mechanisms and implications for changes in the timing of freeze-up.

1.6 Contributions

Chapter 2 was made possible by the help of the co-authors: Andy Mahoney, John Walsh, and Philip Loring. John Walsh provided much help in revisions of the clarity of the manuscript during the peer review process. Chapter 3 is co-authored by Andy Mahoney, John Walsh, Peter Winsor, and Harper Simmons. Chapter 4 is co-authored by Andy Mahoney and John Walsh. Peter Bieniek from the International Arctic Research Center (IARC) provided the WRF-downscaled ERA-Interim wind data, which was used in all three studies. The Arctic Region Supercomputing Center provided access to the Chinook supercomputer which was necessary for all three studies, and technical support.

References

Aksenov, Y., Popova, E. E., Yool, A., Nurser, A. G., Williams, T. D., Bertino, L., and Bergh, J. (2017). On the future navigability of arctic sea routes: High-resolution projections of the arctic ocean and sea ice. *Marine Policy*, **75**, 300–317.

Alaska Ocean Observing System (2018). Ice Detection Buoy. http://www.aoos.org/ice-detection-buoy. Accessed: 2017-07-30.

Ashjian, C. J., Braund, S. R., Campbell, R. G., GEORGE, J. C., Kruse, J., Maslowski, W., Moore, S. E., Nicolson, C. R., Okkonen, S. R., Sherr, B. F., *et al.* (2010). Climate variability, oceanography, bowhead whale distribution, and Iñupiat subsistence whaling near Barrow, Alaska. *Arctic*, pages 179–194.

Barnhart, K. R., Anderson, R. S., Overeem, I., Wobus, C., Clow, G. D., and Urban, F. E. (2014). Modeling erosion of ice-rich permafrost bluffs along the alaskan beaufort sea coast. *Journal of Geophysical Research: Earth Surface*, **119**(5), 1155–1179.

Belchansky, G., Douglas, D., and Platonov, N. (2004). Duration of the arctic sea ice melt season: Regional and interannual variability, 1979–2001. *Journal of Climate*, **17**(1), 67–80.

Brown, J., Jorgenson, M. T., Smith, O. P., and Lee, W. (2003). Long-term rates of coastal erosion and carbon input, elson lagoon, barrow, alaska. In *Eighth International Conference on Permafrost*, pages 21–25.

Cavalieri, D. J., Parkinson, C. L., Gloersen, P., Comiso, J. C., and Zwally, H. J. (1999). Deriving long-term time series of sea ice cover from satellite passive-microwave multisensor data sets. *Journal of Geophysical Research: Oceans*, **104**(C7), 15803–15814.

Cohen, J., Screen, J. A., Furtado, J. C., Barlow, M., Whittleston, D., Coumou, D., Francis, J., Dethloff, K., Entekhabi, D., Overland, J., *et al.* (2014). Recent arctic amplification and extreme mid-latitude weather. *Nature geoscience*, **7**(9), 627.

Comiso, J. C., Parkinson, C. L., Gersten, R., and Stock, L. (2008). Accelerated decline in the arctic sea ice cover. *Geophysical research letters*, **35**(1).

Francis, J. A. and Vavrus, S. J. (2012). Evidence linking arctic amplification to extreme weather in mid-latitudes. *Geophysical Research Letters*, **39**(6).

Francis, J. A., Chan, W., Leathers, D. J., Miller, J. R., and Veron, D. E. (2009). Winter northern hemisphere weather patterns remember summer arctic sea-ice extent. *Geophysical Research Letters*, **36**(7).

Gearheard, S. F., Holm, L. K., Huntington, H., Leavitt, J. M., and Mahoney, A. R. (2017). *The meaning of ice: People and sea ice in three Arctic communities.* International Polar Institute.

Hauser, D. D., Laidre, K. L., Stafford, K. M., Stern, H. L., Suydam, R. S., and Richard, P. R. (2017). Decadal shifts in autumn migration timing by pacific arctic beluga whales are related to delayed annual sea ice formation. *Global change biology*, **23**(6), 2206–2217.

Johnson, M. and Eicken, H. (2016). Estimating arctic sea-ice freeze-up and break-up from the satellite record: A comparison of different approaches in the chukchi and beaufort seas. *Elem Sci Anth*, **4**.

Kohout, A., Williams, M., Dean, S., and Meylan, M. (2014). Storm-induced sea-ice breakup and the implications for ice extent. *Nature*, **509**(7502), 604.

Kovacs, K. M., Lydersen, C., Overland, J. E., and Moore, S. E. (2011). Impacts of changing sea-ice conditions on arctic marine mammals. *Marine Biodiversity*, **41**(1), 181–194.

Long, Z. and Perrie, W. (2012). Air-sea interactions during an arctic storm. *Journal of Geophysical Research: Atmospheres*, **117**(D15).

Mahoney, A., Eicken, H., Gaylord, A. G., and Shapiro, L. (2007). Alaska landfast sea ice: Links with bathymetry and atmospheric circulation. *Journal of Geophysical Research: Oceans*, **112**(C2).

Mason, O. K., Hopkins, D. M., and Plug, L. (1997). Chronology and paleoclimate of storm-induced erosion and episodic dune growth across cape espenberg spit, alaska, usa. *Journal of Coastal Research*, pages 770–797.

Overeem, I., Anderson, R. S., Wobus, C. W., Clow, G. D., Urban, F. E., and Matell, N. (2011). Sea ice loss enhances wave action at the arctic coast. *Geophysical Research Letters*, **38**(17).

Perovich, D. K., Richter-Menge, J. A., Jones, K. F., and Light, B. (2008). Sunlight, water, and ice: Extreme arctic sea ice melt during the summer of 2007. *Geophysical Research Letters*, **35**(11).

Price, J. F., Weller, R. A., and Pinkel, R. (1986). Diurnal cycling: Observations and models of the upper ocean response to diurnal heating, cooling, and wind mixing. *Journal of Geophysical Research: Oceans*, **91**(C7), 8411–8427.

Rainville, L., Lee, C. M., and Woodgate, R. A. (2011). Impact of wind-driven mixing in the arctic ocean. *Oceanography*, **24**(3), 136–145.

Smith, L. C. and Stephenson, S. R. (2013). New trans-arctic shipping routes navigable by midcentury. *Proceedings of the National Academy of Sciences*, **110**(13), E1191–E1195.

Smith, M., Stammerjohn, S., Persson, O., Rainville, L., Liu, G., Perrie, W., Robertson, R., Jackson, J., and Thomson, J. (2018). Episodic reversal of autumn ice advance caused by release of ocean heat in the beaufort sea. *Journal of Geophysical Research: Oceans*.

Stroeve, J., Serreze, M., Drobot, S., Gearheard, S., Holland, M., Maslanik, J., Meier, W., and Scambos, T. (2008). Arctic sea ice extent plummets in 2007. *Eos, Transactions American Geophysical Union*, **89**(2), 13–14.

Stroeve, J. C., Crawford, A. D., and Stammerjohn, S. (2016). Using timing of ice retreat to predict timing of fall freeze-up in the arctic. *Geophysical Research Letters*, **43**(12), 6332–6340.

Taylor, P. K. and Yelland, M. J. (2001). The dependence of sea surface roughness on the height and steepness of the waves. *Journal of physical oceanography*, **31**(2), 572–590.

Toole, J. M., Timmermans, M.-L., Perovich, D. K., Krishfield, R. A., Proshutinsky, A., and Richter-Menge, J. A. (2010). Influences of the ocean surface mixed layer and thermohaline stratification on arctic sea ice in the central canada basin. *Journal of Geophysical Research: Oceans*, **115**(C10).

Yang, J., Comiso, J., Walsh, D., Krishfield, R., and Honjo, S. (2004). Storm-driven mixing and potential impact on the arctic ocean. *Journal of Geophysical Research: Oceans*, **109**(C4).

Chapter 2

Impacts of a lengthening open water season on Alaskan coastal communities: deriving locally-relevant indices from large-scale datasets and community observations

Rolph, R. J., Mahoney, A. R., Walsh, J., Loring, P. A. (2018). Impacts of a lengthening open water season on Alaskan coastal communities: deriving locally relevant indices from large-scale datasets and community observations. *Cryosphere*, **12**(5).

2.1 Abstract

Using thresholds of physical climate variables developed from community observations, together with two large-scale datasets, we have produced local indices directly relevant to the impacts of a reduced sea ice cover on Alaska coastal communities. The indices include the number of "false freeze-ups" defined by transient exceedances of ice concentration prior to a corresponding exceedance that persists, "false break-ups", timing of freeze-up and break-up, length of the open water duration, number of days where the winds preclude hunting via boat (wind speed threshold exceedances), the number of wind events conducive to geomorphological work or damage to infrastructure from ocean waves, and the number of these wind events with on- and alongshore components promoting water set-up along the coastline. We demonstrate how community observations can inform use of large-scale datasets to derive these locally-relevant indices. The two primary large-scale datasets are the Historical Sea Ice Atlas for Alaska and the atmospheric output from a regional climate model used to downscale the ERA-Interim atmospheric reanalysis. We illustrate the variability and trends of these indices by application to the rural Alaska communities of Kotzebue, Shishmaref, and Utqiaġvik (previously Barrow), although the same procedure and metrics can be applied to other coastal communities. Over the 1979-2014 time period, there has been a marked increase in the number of combined false freeze-ups and false break-ups as well as the number of days too windy for hunting via boat for all three communities, especially Utqiaġvik. At Utqiaġvik, there has been an approximate tripling of the number of wind events conducive to coastline erosion from 1979 to 2014. We have also found a delay in freeze-up and earlier break-up leading to a lengthened open water period for all of the communities examined.

2.2 Introduction

2.2.1 Identification of metrics useful for describing climate change-related impacts on Arctic coastal communities

Community engagement and feedback are useful to identify the social relevance of climate system variables commonly used by scientists, as covered extensively by Krupnik and Jolly (2002). For example, sea ice concentration (fraction of an area of ocean surface covered by sea ice), thickness, and extent (ocean area within the sea ice edge) can be considered 'primary' geophysical variables for an Arctic ocean study. However, for indigenous Arctic coastal communities, the timing of local freeze-up and break-up are among the most important characteristics of sea ice (Berkes and Jolly, 2002; Berman and Kofinas, 2004; Laidler *et al.*, 2009). While the definition of freeze-up and break-up timing can vary based on data source (Johnson and Eicken, 2016), it is useful to evaluate these metrics in a way that can be applied across communities, as done in this study. Residents of Arctic coastal communities report that the sea ice is changing in many other ways, including increased presence of rotten (partially melted and weak) ice and the way the ice breaks up (Betcher, personal communication). While these changes are unlikely to be directly captured in climate scale observations, local community members connect these changes with trends that can be indicated from the length of the transition season, or number of false freeze-ups and false break-ups. In

this study, freeze-up day and break-up are defined by the dates when the ice passes a sea ice concentration threshold. The timing at which freeze-up and break-up concentration thresholds are passed does not necessarily imply a phase change, but also can depend on advection of ice driven by winds or currents. While it is difficult to determine the best thresholds in terms of ease of water or ice transportation because the grid cell area covered is larger than the smaller boats or snow machines, concentrations well below 50% are required for navigation by small boats. Serreze *et al.* (2016) use a 30% sea ice concentration threshold, and we adopt that threshold here. The freeze-up and break-up date trends are found in this study (Section 2.4.1) to be similar if the sea ice concentration threshold is 15%, 30% or 45%.

In an analysis framework based on large-scale climate observations, complex inter-connections between communities and the environment can often be overlooked (Huntington *et al.*, 2009). It is therefore important to include local experience when attempting to understand and quantify the impacts of environmental variations and changes (Huntington *et al.*, 2009). As an example drawn upon in this study, Ashjian *et al.* (2010) interviews with Iñupiat whalers in Utqiaġvik (formerly Barrow) identified winds 6 m/s or higher as impediments to whaling because hunters consider the resulting wave conditions too unsafe to travel via boat. Alternatively, Atkinson (2005) used a 10 m/s wind speed threshold for a duration of 6 hours or longer to produce a climatology of storm events. The 10 m/s threshold was based on Solomon et al.'s (1994) finding that winds of this magnitude or greater produce waves with enough power to do geomorphological work on the coastline or damage to infrastructure and habitats. Variations and trends in the number and timing of these events may give an indication of how climate change will impact coastal communities. In this study we present a timeseries of these indices from 1979-2014 (1953-2013 for freeze-up and break-up timing) for three coastal communities in Alaska.

2.2.2 Communities examined in this study

The communities examined in this study are Kotzebue, Shishmaref, and Utqiaġvik. While the locations of the communities vary, all are located along the Alaskan coastline (Figure 2.1) and have community members who participate in coastal or offshore subsistence activities (reliance or partial reliance on marine mammals as a food source and a way of life) (Ashjian *et al.*, 2010; Callaway *et al.*, 1999). The village of Kotzebue is located on a gravel spit on the Baldwin Peninsula, and the population is over 3,500 (NANA Regional Corporation, 2016). Kotzebue Sound has the Noatak, Kobuk, and Selawik rivers providing freshwater seasonally into the Sound. Uses of sea ice in Kotzebue include travel by snowmachine and foot, as well as subsistence hunting from the ice for marine mammals including sheefish and bearded and ringed seals (Georgette and Loon, 1993). Many community members in Kotzebue travel over the ice to transport fuel and goods to summer cabins and communities nearby (Dammann *et al.*, 2018). Historically, the ice offshore has typically broken up in late June and reformed in October.

Shishmaref is located on a Chukchi Sea barrier island, about 0.25 miles wide and 3 miles long, slightly north of the Bering Strait and about 100 miles southwest of Kotzebue. It is at the cen-

ter of animal migration routes and also a center of a complex food-distribution system based in subsistence hunting practices (Marino, 2012). The community members of Shishmaref hunt the subsistence animals of seals and walrus (Huntington *et al.*, 2017). It is highly vulnerable to erosion, which has been exacerbated by declining sea ice cover protecting the coastline (Barnhart *et al.*, 2014b). Hunters use sea ice as a platform for transportation, and the hunters of Shishmaref have indicated that there are no longer large pressure ridges to hold the ice in place, which makes the spring sea ice break up more quickly, and so more dangerous to travel on (Huntington *et al.*, 2017). The members of Shishmaref have voted twice to permanently relocate the village due to this problem, however the funds are not available for doing so, even though the community will eventually have to move (Department of Commerce, Community, and Economic Development, 2017). The sea ice typically breaks up earlier than at Kotzebue, around May, and freezes up later, around November.

Utqiaġvik (formerly Barrow) officially reverted back to its original name in December 2016. It is the largest village on the North Slope Borough in Alaska and is located along the Chukchi Sea. Utqiaġvik is in a highly exposed position for drifting pack ice and also land-fast ice. Freeze-up has historically been in October or early November, and break-up can last from April through August (Johnson and Eicken, 2016). Sea ice in Utqiaġvik can be a hazard for commericial shipping, and it serves as a platform for the hunting of subsistence animals. Seal hunting can take place on the ice in winter, and bowhead whale hunting is done from the edge of land-fast ice in spring and from open water in fall (Gearheard *et al.*, 2006).

2.2.3 Organization of this paper

This paper is organized into the following sections. First, we describe the Data and Methods, which are separated into subsections describing the Historical Sea Ice Atlas and downscaled ERA-Interim datasets, sources of community observations, the rationale for the selection of the study areas, and descriptions of the locally relevant metrics of the changing sea ice conditions in these communities. We then present the results showing how these metrics have been changing for each community. All the indices have been evaluated for the time period from 1979-2014. For the freeze-up and break-up dates, we evaluated a longer time period of 1953-2013. Next, the Discussion section links these indices to actual and potential impacts on the selected communities, including impacts on travel for subsistence hunting, prey availability, and erosion. Finally, the Conclusion section briefly summarizes our main findings.

2.3 Data and Methods

2.3.1 The Historical Sea Ice Atlas

The Historical Sea Ice Atlas (HSIA) for Alaska contains monthly gridded fields of sea ice concentration extending back to 1850. As described by Walsh *et al.* (2017), it is a synthesis of various datasets ranging from whaling ship logs to historical ice chart archive products to the passive microwave data for the more recent decades (1979-2017). A full list of all sources of data into the

HSIA can be found on the Scenarios Network for Arctic and Alaska Planning (SNAP) webpage (http://seaiceatlas.snap.uaf.edu/about). Temporal interpolation and analog reconstructions of months with missing data fill any gaps in the dataset. From 1953 through 2013, quarter-monthly sea ice concentration values are available and were used here to construct the sea ice indices and to analyze their trends along the coastlines of the selected communities in Alaska. The quarter-monthly grids were assigned calendar dates by the best approximation of the midpoint day of each quarter-monthly file. Use of HSIA data roughly doubles the timespan of the data available with sub-monthly temporal resolution compared with a reliance solely on the sea ice data derived from the satellite passive microwave record, which begins in 1979. While the satellite-derived (post-1979) portion of the dataset is less susceptible to heterogeneities arising from the use of multiple data sources, we do not find evidence for spurious discontinuities around 1979.

2.3.2 WRF-downscaled ERA Interim reanalysis products

The European Centre for Medium-Range Weather Forecasts interim reanalysis (ERA-Interim) dataset (Dee *et al.*, 2011) has been dynamically downscaled using the Advanced Research version of the Weather Research and Forecasting (WRF) regional model (Bieniek *et al.*, 2016). The dataset has an hourly temporal resolution (daily for sea ice) and a 20 km spatial resolution, from 1979-2014. It has been downscaled from a 0.75 degree (about 83 km) spatial and 6 hourly temporal resolution of the ERA-Interim reanalysis. The regional model simulation is observationally constrained by a reinitialization to the ERA-Interim reanalysis every 48 hours. Sea ice concentration is prescribed (and spatially interpolated) from the ERA-Interim reanalysis, which in turn obtained its sea ice information from satellite passive microwave sources. The downscaling was performed in order to improve representation of temperature and precipitation around Alaska's varying terrain, and to inform various stakeholders with higher-resolution climate and weather information. The WRF regional model uses a thermodynamic sea ice model of Zhang and Zhang (2001), together with the Noah land surface model, to simulate the surface fluxes over sea ice and land areas, respectively. As discussed in the following subsection, we used the sea ice concentrations and wind data from grid cells offshore the selected communities of Kotzebue, Shishmaref, and Utqiaġvik (Figure 2.1).

2.3.3 Selection of grid cells representative of each study area

The communities of Kotzebue, Shishmaref, and Utqiaġvik were selected to represent a range of sea ice states and vulnerability to coastal erosion. The three communities have varying levels of reliance on subsistence activites and interaction with the offshore oil and gas industry. Figure 2.1 shows the grid cells selected for each community, for comparison of sea ice metrics. To assess variability of ice conditions, we selected data near but not adjacent to the coastline of each community due to the fact a large part of the sea ice dataset is satellite-derived. Satellite-derived sea ice concentration data have difficulty resolving sea ice in pixels immediately adjacent to the coastline. This can cause problems in obtaining accurate sea ice concentrations in the model grid cells adjacent to the coastline, as these grid cell values are interpolated from the satellite-derived

concentrations prescribed from ERA-Interim. For example, there is a common flaw lead system south of the grid cells selected for Utqiaġvik, which develops during winter and spring (Norton and Gaylord, 2004). For the above reason, selecting "coastally contaminated" grid cells closer to shore would likely not improve representation of the sea ice conditions. The reliance on offshore ice concentrations highlights the need for across-community datasets containing reliable sea ice concentrations close to shore.

The maximum concentration (greatest fraction of sea ice per unit area) was extracted from a six-gridcell area offshore of each community. The maximum (rather than the six-cell average) concentration was extracted because the grid cell with the highest concentration can serve as a "choke point" or hazard, while the other grid cells may not. However, in an analysis over the entire seasonal cycle, we found that neighboring grid cells offshore from the coast do not typically vary significantly in concentration. The location selected for the analysis of downscaled wind speed data were selected slightly further offshore in order to get a better representation of open ocean travel, but the results in terms of open water days are similar to those obtained from the HSIA analysis.

2.3.4 Indices related to freeze-up, break-up, and duration of open water period

In the analysis that follows, we define freeze-up and break-up as the seasonally "final" crossings of a given ice concentration threshold. The open water period is defined as the duration between freeze-up and break-up, when ice concentration stays continuously below this threshold. We experimented with different concentration values and found that the resulting dates of freeze-up and break-up are relatively insensitive to thresholds between 15% and 30%. To illustrate this, we used a threshold of 30% for the HSIA data, as used by Serreze et al. (2016), and a threshold of 15% as used by NSIDC, for the ERA-Interim data (Figure 2.2).

A "false break-up" is defined to occur when the ice concentration dips below the threshold before the final break-up prior to the open water season of that calendar year. Similarly, a "false freeze-up" is defined to occur when the sea ice concentration threshold rises above the threshold concentration between the final break-up and the final freeze-up of that calendar year. The numbers of false freeze-ups and false break-ups were also calculated for each community. The downscaled ERA-Interim data were used for these calculations because temporal resolution of ERA-Interim is finer than that of HSIA (daily instead of quarter-monthly). Because the ERA-Interim concentrations were used, the evaluation of false break-ups and false freeze-ups spanned the period 1979-2014.

2.3.5 Indices relating to open-water wind events

The number of 'boatable' open water days refers to the number of days that sea ice concentration is below 15% while the winds do not exceed a 6 m/s threshold. This threshold is based on hunting success of whalers in Utqiaġvik (Ashjian *et al.*, 2010). Besides a wind speed threshold, on St. Lawrence Island, wind direction has been shown to be an important factor for hunting walrus,

and can cause heavy ice conditions close to shore making it difficult to launch boats (Kapsch *et al.*, 2010). Savoonga and Gambell have higher recorded average wind speeds for their hunting days (5 to 9 m/s) than Utqiaġvik (Kapsch *et al.*, 2010). Higher winds speeds are usually considered by the hunters to be dangerous to hunt via boat. Ashjian et al. identified the 6 m/s wind speed threshold from interviews with 41 Iñupiat whale hunters and found that 86% of fall whales in Utqiaġvik were landed on days where the wind speed was less than 6 m/s, while no whales were landed on days where winds exceeded 10 m/s.

Wind events exceeding 10 m/s for a duration of 6 hours of longer have been found to have potential to cause geomorphological change, or damage to coastal infrastructure or habitats (Atkinson, 2005; Jones *et al.*, 2009). The number of these events were calculated for Kotzebue, Shishmaref, and Utqiaġvik from 1979 through 2014 using the WRF-downscaled output. Timesteps of lulls during 'shoulder events' were counted as part of the geomorphologically-significant wind event as long as the wind speeds did not dip below 7 m/s, which follows the same method as used in Atkinson (2005). We have also counted the number of high wind events as defined by Atkinson (2005) (greater than 10 m/s for at least 6 hours), but have an added restriction that winds conducive to erosion must be blowing from directions within a 90-degree arc between normal to the coastline and alongshore with the coast to the right of the wind. High winds from these directions favor both wave generation and water setup along the coastline (i.e. increase in local sea level), and can therefore be particularly damaging to a community in terms of increasing erosion rates (Barnhart *et al.*, 2014a) and possible infrastructure damage due to flooding. Winds from between 225° and 315° satisfy both the alongshore and onshore requirements at Utqiaġvik. Winds blowing from directions between 180° and 270° satisfy the criteria for Kotzebue, while Shishmaref's quadrant ranges from 225° and 315°.

2.4 Results

2.4.1 Changes in timing of freeze-up and break-up, and number of false freeze-ups and break-ups

The HSIA dataset was used in order to extend the timeseries of freeze-up and break-up timing for the communities of Kotzebue and Shishmaref 27 years prior to the starting date of purely satellite-derived datasets. For years which showed multiple freeze/break events, the final freeze-up and break-up date was used. The linear trend of the date of freeze-up is a delay of 2.2 days per decade for Kotzebue and 6.0 days per decade for Shishmaref (Figure 2.3). The freeze-up day for Kotzebue Sound shows a much weaker trend than the freeze-up days for Shishmaref. As shown in Figure 2.4, break-up has occurred earlier by 3.4 days per decade at Shishmaref, and by 1.1 days per decade at Kotzebue. However, the interannual variability of the freeze-up and break-up dates is sufficiently high that none of these trends are statistically significant at the 5% level. Utqiaġvik's trends in freeze-up and break-up timing since 1953 (HSIA data) are not shown because there are a high number of years with no freeze-up and break-up date as defined by a 30% threshold, since the sea ice concentration remained higher year-round.

Not only are there differences in the trends of freeze-up and break-up between the selected communities, but the variance is different as well (Table 2.1). The variance of the freeze-up date is 32% larger at Kotzebue than at Shishmaref, and the variance of the break-up date is 8% larger at Kotzebue than at Shishmaref. Fractions of the variance that are explained by the trend are 6% and 2% for the freeze-up and break-up day of Kotzebue, and much higher for Shishmaref: 44% and 20% for freeze-up and break-up date respectively. The smaller percentages at Kotzebue imply that the trend will be a poorer guide to future break-up and freeze-up dates than at Shishmaref.

There has been an increase in recent years in the number of false freeze-ups and false break-ups at all three communities (Figure 2.5). There have been more false break-ups than false freeze-ups for both Kotzebue and Utqiaġvik. In contrast, Shishmaref shows many more false freeze-ups than false break-ups: 17 false freeze-ups from 2002-2014, with only 6 false break-ups. In prior decades (1979-2001), Shishmaref had only 2 false freeze-ups and no false break-ups. Kotzebue also shows an increase in the number of false freeze-ups and break-ups in recent years, with none prior to 2004. However, from 2004-2014, Kotzebue had 5 false freeze-ups and 9 false break-ups. Utqiaġvik shows 5 false freeze-ups in recent years (2002-2013), with 15 false break-ups. There were only 3 false break-ups prior to 2002, with 3 false freeze-ups.

2.4.2 Changes in the number of days 'too windy' for safely hunting via boat

The average number of boatable days (based on the definition provided by Ashjian *et al.* (2010)) from 1979-2014 in Kotzebue is 87.0 days, while in Shishmaref the average number is 79.2 days. Utqiaġvik shows an average of 32.0 boatable days for the same time period. The number of 'boatable' days in the open water period is not increasing as rapidly as the total number of open water days because some of the open water days have winds exceeding the 6 m/s criterion for safe boating. This is especially true at Utqiaġvik, where the number of unboatable open water days is increasing at a rate of 1.4 days/year with an r^2 value of 0.49 (Figure 2.6). The rate of total increase in open water days is 2.5 days/year with a similar r^2 value of 0.47. The increases in both total number of open water days and unboatable days are statistically significant. Shishmaref and Kotzebue show only weak and statistically insignificant increases in the number of windy days over open water (Figure 2.7). Kotzebue has a statistically insignificant increasing trend of the total number of days without ice cover (4.2 days per decade), while the trend in Shishmaref is statistically significant (5.6 days per decade). Shishmaref, on average, shows more unboatable days than Kotzebue, but Shishamref also shows a higher number of open water days in general. Although Kotzebue has an overall lower number of days of open water, there is a higher number of days for community members to hunt via boat.

2.4.3 Increasing number of wind events with potential for geomorpholgical change

As described in Section 2.3.5, wind events exceeding 10 m/s for at least 6 hours have the potential to cause geomorphological change (Atkinson, 2005; Solomon *et al.*, 1994; Jones *et al.*, 2009). The number of such events over open water have been increasing, particularly at Utqiaġvik (Figure

2.8). The rate of increase in the number of geomorphologically significant wind events over open water near Utqiaġvik is about 1 every 2 years, with an r^2 value of 0.2, approximately tripling the number of wind events (10 to 30 events) over the 36 year time period from 1979-2014. There has also been a change in the character of the time series. Between 1993-2014, some years (e.g. 1983, 1985, 1988, 1991, and 1992) did not have any of these wind events over open water, because the ice pack did not recede far enough offshore in earlier years. At Kotzebue, there has also been an increase in geomorphologically significant wind events, but at a slower rate than Utqiaġvik, about 1 additional event every 5 years, leading to an increase of about 7.2 events over the 36 year time period (Figure 2.8). Shishmaref shows the weakest increase in the total number of high-wind events (including all directions), about 1 every 10 years. Despite this weaker trend, Shishmaref has a higher number of such events than Kotzebue. Over the 36 year time period examined, Kotzebue has had an approximate increase from 39 to 46.2 total wind events, while Shishmaref has seen an increase from an average of 49 to 52.6 events.

In addition, wind direction is very important to determine if a particular wind event is able to set up water along the coastline enough to cause flooding, increased coastal erosion, or infrastructure damage (Barnhart *et al.*, 2014b). The average number of high-wind events from the quadrant favorable for erosion at Utqiaġvik is approximately 4.6 with a significant increasing trend of 0.14 per year. The maximum number of these events is 14, and the minimum is 0 for Utqiaġvik. If we count only the number of wind events exceeding 10 m/s for at least 6 hours, and coming from between 315° and 225°, the annual average of Shishmaref is 7.22, with a minimum of 1 and a maximum of 14, with no significant trend. At Kotzebue, the average number of onshore wind events is 6.61, with a maximum of 12.0 and a minimum of 2.0. At Utqiaġvik, the annual percentages of the total hours during these on- and along-shore high wind events (between 225° and 315°, see Section 2.3.5) average at 21%. At Kotzebue, an average of about 12% of the winds above 10 m/s were onshore and between 180° and 270° during 1979-2014. An average of about 9% of the total duration of the high wind events in Shishmaref were from between 315° and 225°, which are the directions conducive to increased levels of erosion and flooding.

2.5 Discussion: Impacts and Implications

2.5.1 Consequences of changes in the transition period between open water and ice: Timing and number of freeze-up and break-up events

Our results show that in all three communities the annual number of open water days has increased in recent decades (Figure 2.2) due to increasingly delayed freeze-up (Figure 2.3) and earlier break-up (Figure 2.4) of the ice cover. Additionally, the twice-annual transitions between open-water and ice-covered seasons are becoming increasingly ill-defined and characterized by multiple "false" freeze-up and break-up events before the final, lasting transition occurs (Figure 2.5). According to our definitions of these events (see Section 2.3.4), false freeze-ups and break-ups were non-existent in Kotzebue prior to 2004, after which they have occurred with some regularity (Figure 2.5a,d). In Shishmaref, two false freeze-ups occurred in the 1980s, but since 2002 they have

occurred more often than not and most often multiple times per year (Figure 2.5b). False transition events appear to have been more common in Utqiaġvik overall (Figure 2.5c,f), but there has been a marked increase in the number of false break-ups in the last decade. These results are in agreement with local observations by residents of Arctic communities, such as those of one community member from Kotzebue who reports "we have a longer fall and a longer spring so it's warming on both ends and the winter is getting shorter ... used to be everything would melt in one week" (Betcher, personal communication, 2013). Freeze-up and break-up represent important events in the cultural calendars of coastal communities in the Arctic (Gearheard *et al.*, 2013) and these changes therefore have significant consequences for residents and their subsistence activities. However, the nature and severity of these consequences depends upon the local ice regime and cultural practices, and each community must therefore be considered individually.

Once the ocean surrounding the community starts freeze-up, transportation via small boats becomes increasingly difficult and risky. Hence, until a stable landfast sea ice cover forms (allowing the use of snow machines, dog-sleds, or regular street vehicles in some cases) early winter travel to the mainland from villages on islands and peninsulas such as Shishmaref and Kotzebue can be extremely limited. The growing number of false freeze-up events each year extends this period of reduced accessibility and increases the level of uncertainty at this time of year. In the Canadian Arctic community of Igloolik, Laidler *et al.* (2009) report that "hunters are finding autumn sea ice travel more dangerous, travel routes must be altered, and people are essentially stuck in town" during this period. In Utqiaġvik, travel to inland hunting regions or other communities is not directly affected by sea ice conditions, but boating during the extended open water season has been impacted by winds and waves. This is discussed in more detail in section 2.5.2.

Entrainment of sediments by sea ice commonly happens during the formation of sea ice in shallow water. Sediment entrainment (Eicken *et al.*, 2005) could therefore potentially increase with an increasing number of coastal freeze-up events in a given year. The reduced albedo of sediment-laden ice (Light *et al.*, 1998) promotes subsequent melt and early break-up the following year. Ice shove events, during which sea ice piles or rafts onto the shore, are another coastal process that may be impacted by the number of false freeze-ups. They occur most commonly in the fall and spring (Kovacs and Sodhi, 1980) and represent a significant hazard in some Arctic coastal communities. With an increasingly delayed freeze-up extending into the fall storm season (see section 2.5.3), and a higher number of false freeze-ups happening at the same time, it seems possible that coastal communities may also experience more ice shoves.

The subsistence harvests of all Arctic coastal communities include ice-associated marine mammals such as ringed and bearded seals, walrus, belugas, and bowhead whales (Moore and Huntington, 2008). The availability and accessibility of each of these species, in terms of both the population size and proximity to hunting grounds, will be impacted by changes in the timing and persistence (number) of freeze-up and break-up events. Work done by Kapsch *et al.* (2010) identified optimal conditions for maximum walrus hunting success in St. Lawrence Island, Alaska, of 0 to 30% ice concentration, and specific windows of wind speeds, temperature, and visibility. This

suggests that a delayed freeze-up will shift the optimal walrus hunting conditions to later in the year, though Kapsch *et al.* (2010) found that hunting success was more sensitive to ice conditions in spring than fall. Interviews collected by Krupnik and Jolly (2002) indicate that open water can be a driver of early break-up, and can make walrus hunting difficult.

In Utqiaġvik, the spring whale harvest traditionally take place in the lead that forms at the seaward edge of the landfast ice with the butchering taking place on the landfast ice itself (e.g. Gearheard *et al.*, 2013). Although the grid cells selected for our study do not capture landfast ice at Shishmaref and Utqia ˙gvik, Mahoney *et al.* (2014) found trends toward earlier break-up of landfast ice along the Alaska coast in agreement with those identified here. These changes reduce the time for which landfast ice is available as a platform for spring whaling. Without landfast ice, communities must butcher their catch on the beach, which creates additional challenges for disposal of the carcasses.

Ringed seals are ice-associated year-round, and breeding occurs on stable ice with good snow cover. If a delayed freeze-up (Figure 2.3) or an increased number of freeze-up/break-up events (Figure 2.5) means there is less time for the snow cover to develop, pups are more exposed to predators due to inability to construct an adequate lair (Kovacs *et al.*, 2011). Ringed seals can be hunted for subsistence whenever ice is accessible, either on landfast ice or among loose floes by boat (Gearheard *et al.*, 2013), but the overall accessibility to subsistence hunters is reduced by the shortening of the ice-covered season. Bearded seals are also likely to be negatively impacted by an earlier break-up (Figure 2.4), because they require stable seasonal ice late in the spring for raising pups and moulting (Kovacs *et al.*, 2011). Ideal hunting conditions consist of loose floes accessible by small boats. These conditions typically occur as the ice is in the process of breaking up and hence the occurrence of multiple break-up events each year may potentially offer increased hunting opportunities. However, the overall earlier occurrence of break-up means an earlier start to the hunting season, which may conflict with other subsistence activities or become out of sync with the life events of the seals.

2.5.2 Increases in open water duration and the number of windy days over open water

As a result of a delayed freeze-up and early break-up, the open water season has lengthened at all three communities, though most rapidly at Utqiaġvik (Figure 2.2). Using the HSIA dataset, we see that this change began abruptly in the late 1990s (Figure 2.9), when the summertime sea ice edge first began retreating significantly to north of Point Barrow. As the northernmost tip of Alaska, once the sea ice has retreated beyond Point Barrow, navigation to points further east along the northern Alaska and Canadian coasts becomes possible. Consequently, the recent changes in the length of the open water season at Utqiaġvik (Figures 2.6, 2.7, and 2.9) have led to a significant increase for maritime traffic destined for Utqiaġvik or locations further east (Smith and Stephenson, 2013). Longer navigation seasons along other Arctic coasts are leading to an increased use of coastal shipping routes and development of offshore continental shelves (Instanes *et al.*, 2005). However, it should also be noted that as sea ice retreats, the resulting larger fetch of open water is

likely to lead to increased wave height (Thomson and Rogers, 2014). Additionally, without deep water ports or protective breakwaters, swell propagating through open water may prevent barges from offloading goods even under calm winds. Associated political, economic, and social consequences for residents of Arctic coastal areas could be significant and possibly outweigh direct physical impacts from global warming.

In addition to extending the navigation season, the lengthening open water season allows for more time for winds to impart momentum to mix the upper ocean and create waves. Wind waves represent a significant hazard for hunters in small boats, who may need to travel further from shore to obtain their catch in recent years. Aerial surveys in the western Beaufort Sea indicate that as the ice retreats further from shore, bowhead whales are travelling closer to the coast during their fall migration (Druckenmiller *et al.*, 2017), but hunters in Utqiaġvik reported during interviews that they had to travel farther from land due to increased barge activity pushing whales out further from shore. This is an example of the complex interplay of social systems responding to environmental change. Hunters stress that whales should be harvested closer to the community so the meat does not spoil on the haul back to shore (Ashjian *et al.*, 2010).

The problem of traveling further from shore is amplified by an increase in the annual number of high wind events over open water (Figures 2.6, 2.7c, and 2.8) which will lead to more days with high waves. The trends of number of boatable open water days in conjunction with the increase in total number of open water days should be taken into account when examining the impacts of climate change on subsistence activities taking place from boats. The open water season has increased 4.2, 5.6, and 25 days per decade for Kotzebue, Shishmaref, and Utqiaġvik respectively, but the number of boatable days has increased by 1.2, 3.1, and 10.7 days/decade for each community, also respectively. The increase in the number of open water days at all communities agree well with the results of Parkinson (2014). Greater wave heights caused by increased fetch can hinder hunting success much more than prey abundance due to lack of access to the prey. Hansen *et al.* (2013) examined threshold wind speeds reported by Wainwright hunters which were deemed unsafe hunting conditions. 11% fewer boatable days was determined for bowhead whales in spring (15 April - 15 June) and 12% in summer (1 July - 31 August) over the period 1971-2010. In terms of handling larger waves due to increased fetch and the increasing amount of time open water is exposed to storm activity, perhaps hunters can obtain access to more stable, suitable, and bigger boats. The impacts of climate change and changes in the timing of freeze-up and break-up might be less severe if communities are able to adapt their hunting practices effectively.

2.5.3 Increasing winds over open water: Number of geomorphologically significant wind events and consequences for erosion

It is well documented that a lengthened period of open water leaves Arctic shorelines more vulnerable to erosion from autumn storms (Barnhart *et al.*, 2014b; Overeem *et al.*, 2011). Moreover, along the Alaskan coast during the open water period, we have found the number of wind events capable of doing geomorphological work or creating hazards to habitat or infrastructure (as de-

fined by Atkinson (2005)) is increasing at all three communities in this study (Figure 2.8). The trend is strongest along the northern coast near Utqiaġvik, although the number of events annually is significantly less than we find at Kotzebue and Shishmaref. Once we apply an additional wind direction criteria to count only those events likely to produce both waves and coastal setup, we see a substantially lower number of events and we find that Utqiaġvik is the only community to exhibit a significant increasing trend in these wind events. Shishmaref shows the highest number of the high wind events coming from the direction allowing for water set up along the coastline, and although no significant increasing trend was found, these events contribute to an already existing problem of shoreline erosion there. Kotzebue shows only a slightly lower annual average of these water set-up events than Shishmaref, but differences in the geographical location of the communites should also be considered in terms of relative exposure to the open ocean and increases in fetch. Shishmaref is more exposed to the open ocean than Kotzebue because it is not geographically located within a Sound, and this might also contribute to differences in water setup along the coastline. Closely monitoring possible future trends in these events for all communities can provide a proxy for future shoreline erosion.

Parkinson and Comiso (2013) presented a quantifiable variation of coastline exposure due to inconsistencies in trends of the delayed freeze-up and earlier break-up of sea ice, but this study analyzed years starting with the satellite era in 1979. By using HSIA data, we were able to quantify changes in the duration of the open water period offshore Utqiaġvik since 1953 (Figures 2.9), before the satellite data became available. Although there are other factors that influence coastal erosion rates (e.g. permafrost extent, surface geology), a change in the number of wind events able to geomorphological work, and how often the winds in these events have directions favorable to increased water levels, may also be an indicator of how vulnerable a particular coastline is to erosion. An increase in these wind events which can create significant storm surge can also be a threat to food security. For example, in Shishmaref, an October 1997 storm caused 30 ft waves and swept away multiple families' winter supply of food which was stored on top of permafrost, but under sand. In addition to food storage locations, multiple homes have had to be relocated and school housing, a warehouse, and a tannery were also threatened (Callaway *et al.*, 1999).

2.6 Conclusions

By applying simple thresholds identified using local observations, we have demonstrated that large-scale climate datasets can be used to assess the impacts of a changing climate to the three Alaska coastal communities of Kotzebue, Shishmaref, and Utqiaġvik. The methods used in this study can be applied to any Arctic coastal community, though the specific thresholds and impacts of changes are likely to differ. Our results show differences in changes of the sea ice regime across the three communities. Particularly Utqiaġvik is showing the most pronounced changes in terms of a lengthening open water season. However, changes in the open water period are not able to capture the full story of the impacts of changes in sea ice cover, as we have demonstrated in this study. Other indices specific to individual communities and informed by local knowledge must

be used.

The number of 'boatable' open water days is not increasing as much as one might expect from the lengthened open water period, particularly in Utqiaġvik. Some of the additional days in the open water period occur during the fall storm season when there commonly are days too windy for hunting or travel by boat. Therefore, lost days during the ice covered season that might have been suitable for snow machine travel are not necessarily offset by an equal number of boatable days.

Lengthening of the open water season has been linked to increased rates of coastal erosion (Overeem *et al.*, 2011). Our results show that the number of wind events capable of performing significant erosion (Atkinson, 2005; Solomon *et al.*, 1994) scales with the length of the open water season. Accordingly, Shishmaref, which has an open water season approximately twice that near Utqiaġvik, also has approximately twice as many erosion-capable wind events. All three communities showed positive trends in the number of such events, but Utqiaġvik showed the strongest increase over the study period, with roughly three times the number of events in 2014 as occurred in 1979. The trend at Utqiaġvik is still apparent when we consider only those high wind events coming from directions favoring both onshore wave generation and coastal set up (i.e. from the NW and SW). If this trend continues, erosion rates are likely to increase in the future at Utqiaġvik, placing the community's substantial (compared to the other Arctic coastal communities) coastal infrastructure at risk.

Along with the increases in open water season length, our results also show that the number of false freeze-ups and false break-ups has increased substantially in recent years. As a result, community members are finding it more difficult to change modes of transportation with the seasons. During the intervals between false transition events, coastal residents can be trapped without a reliable method of transportation (Laidler *et al.*, 2009). Although Utqiaġvik is showing a greater increase in the number of open water days, Shishmaref has had the greatest increase in the number of false freeze-ups in recent years according to ERA-Interim data. Kotzebue experiences the fewest false freeze-up and break-up events, but they did not occur before 2004. If the patterns of the more recent years continue, the occurrence of false freeze-ups and break-ups could begin to define a new 'normal' for the transition periods between open water and sea ice cover.

Indices such as those we have derived here show that the use of community observations and local knowledge in conjunction with large-scale climate datasets can be a powerful tool in evaluating the impacts of climate change at local scales. All of our results relied on the use of a sea ice concentration threshold to identify transitions between periods of open water or ice cover. For further research, it would be useful for individual communities to report when freeze-up and break-up occur. If every community provided this information, choosing a threshold for sea ice concentration may not be required in terms of comparing analysis of large-scale datasets across communities.

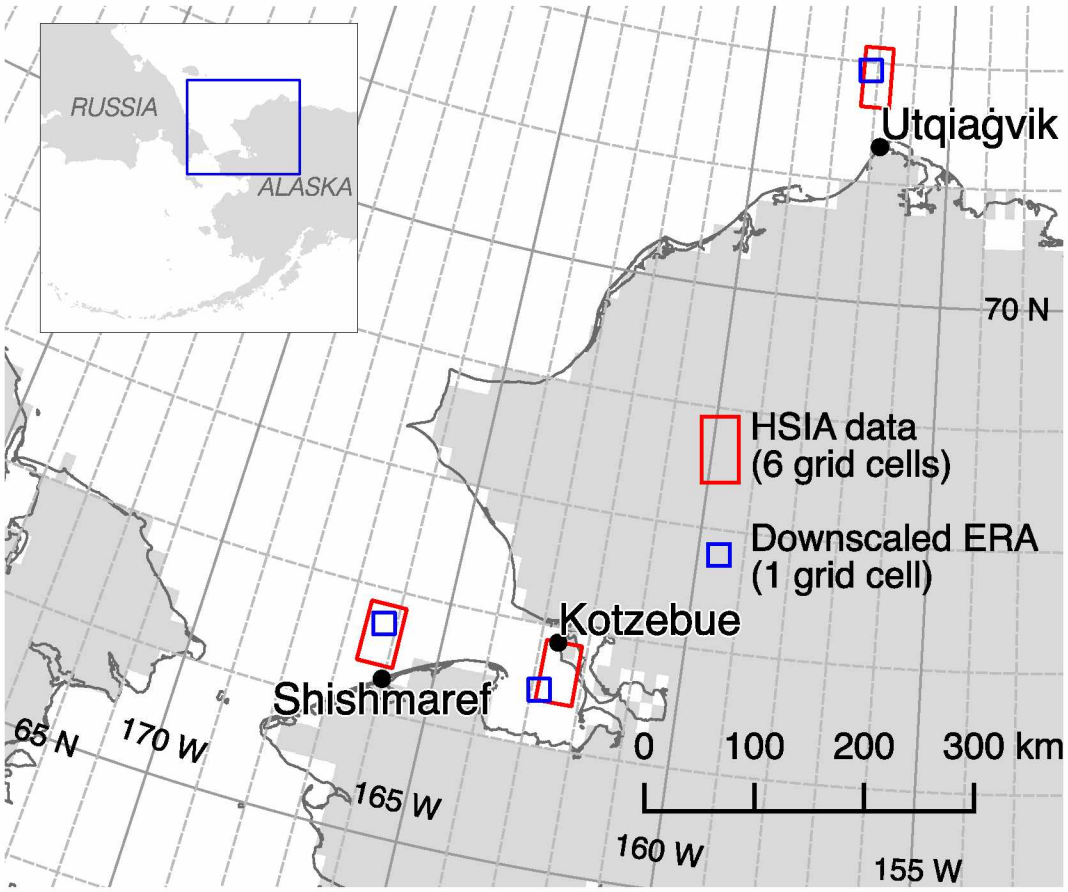

Figure 2.1: Selected grid cells from the Historical Sea Ice Atlas and WRF-downscaled ERA-Interim datasets used to extract sea ice concentration (also wind speeds from the WRF-downscaled dataset) offshore several communities.

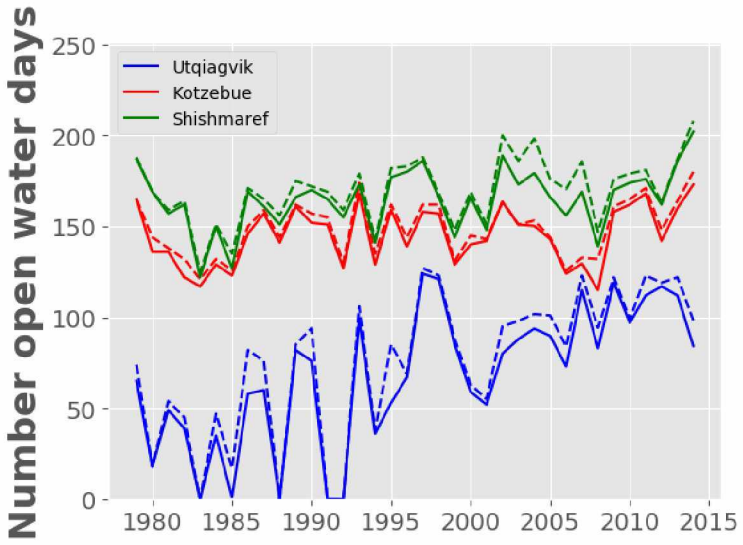

Figure 2.2: The number of open water days are similar if a 15% (solid line) or 30% (dashed line) sea ice concentration threshold is used. If the sea ice concentration (area of the grid cell) is lower than the threshold value, it is considered open water. Sea ice concentrations for the communities are extracted from the grid cells labelled as "Downscaled ERA" in Figure 2.1.

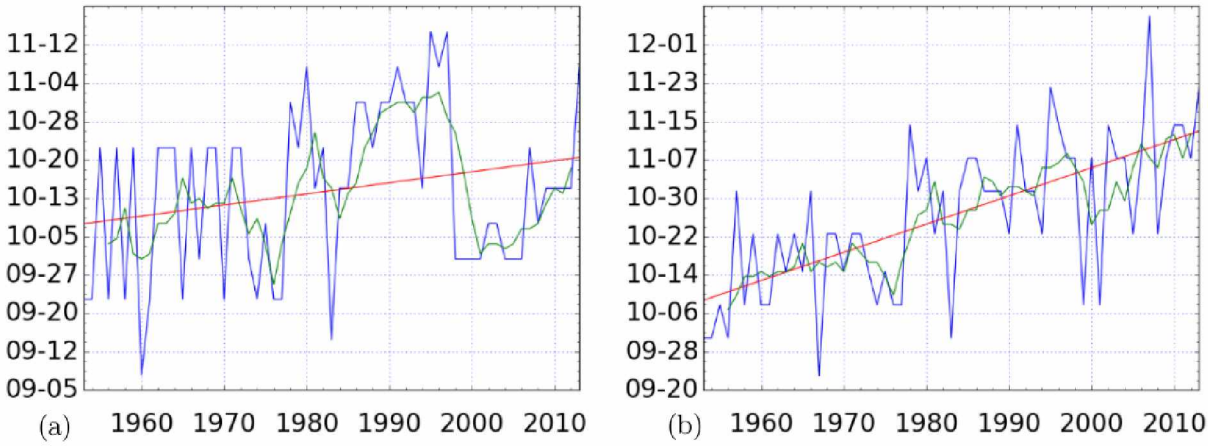

Figure 2.3: Trends in freeze-up day of year for (a) Kotzebue and (b) Shishmaref. Blue line is yearly freeze-up day, and green line indicates the 5-year running mean. Data from HSIA.

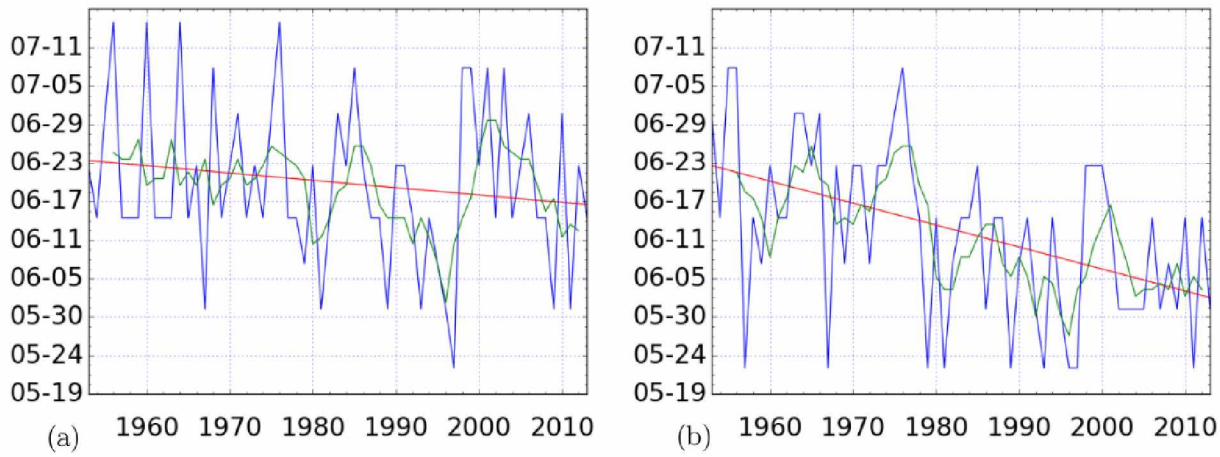

Figure 2.4: Trends in break-up day of year for (a) Kotzebue and (b) Shishmaref. Blue line is yearly break-up day, and green line indicates the 5-year running mean. Data from HSIA.

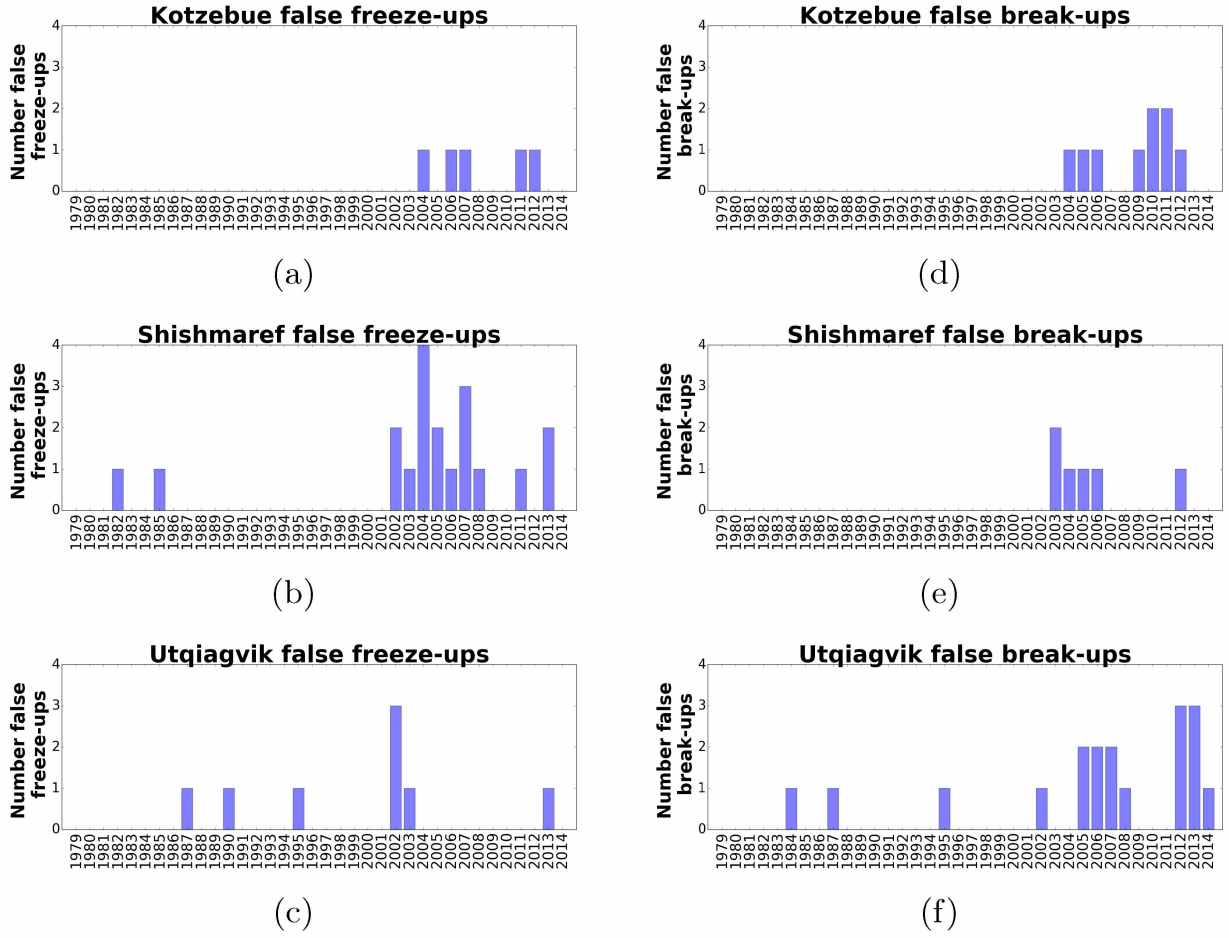

Figure 2.5: The number of false freeze-ups and break-ups per year, identified by ERA-I daily sea ice concentration data. False freeze(break)-ups are defined as the number of times the ice concentration oscillated above and below the sea ice concentration threshold value of 15% before the last freeze(break)-up was finally achieved.

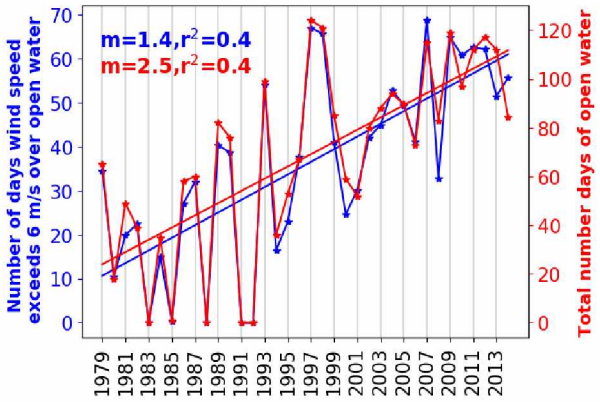

Figure 2.6: Annual timeseries from 1979-2014 of the number of days deemed too windy for boat travel for subsistence hunting (> 6 m/s, (Ashjian et al, 2010)) and number of open water days (number of days less than 15% sea ice concentration). Data from WRF-downscaled ERA-Interim.

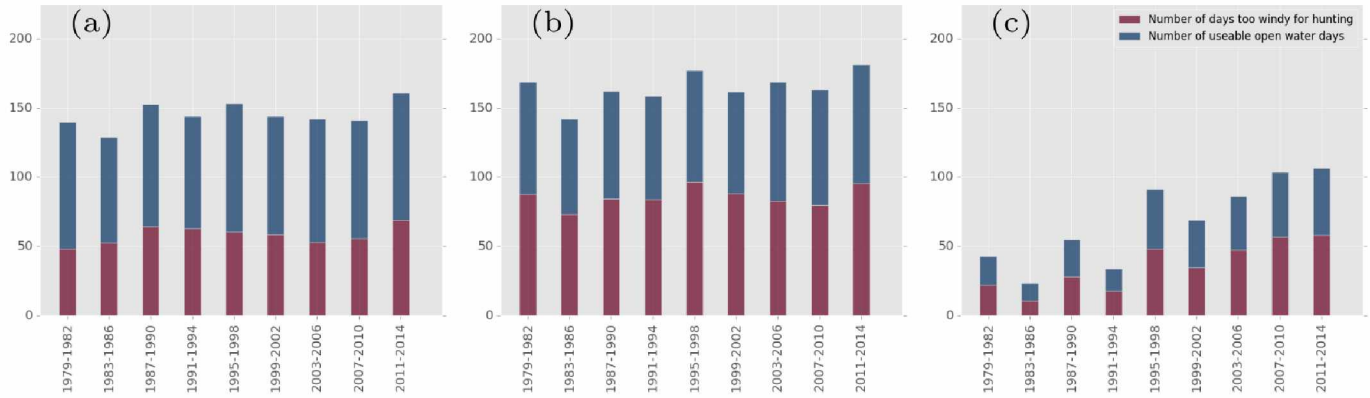

Figure 2.7: The number of days deemed too windy for boat travel for subsistence hunting (> 6 m/s, (Ashjian et al, 2010)) with the number of open water days (number of days less than 15% sea ice concentration) for (a) Kotzebue (b) Shishmaref and (c) Utqiaġvik. Data taken from the WRF-downscaled ERA-Interim Reanalysis.

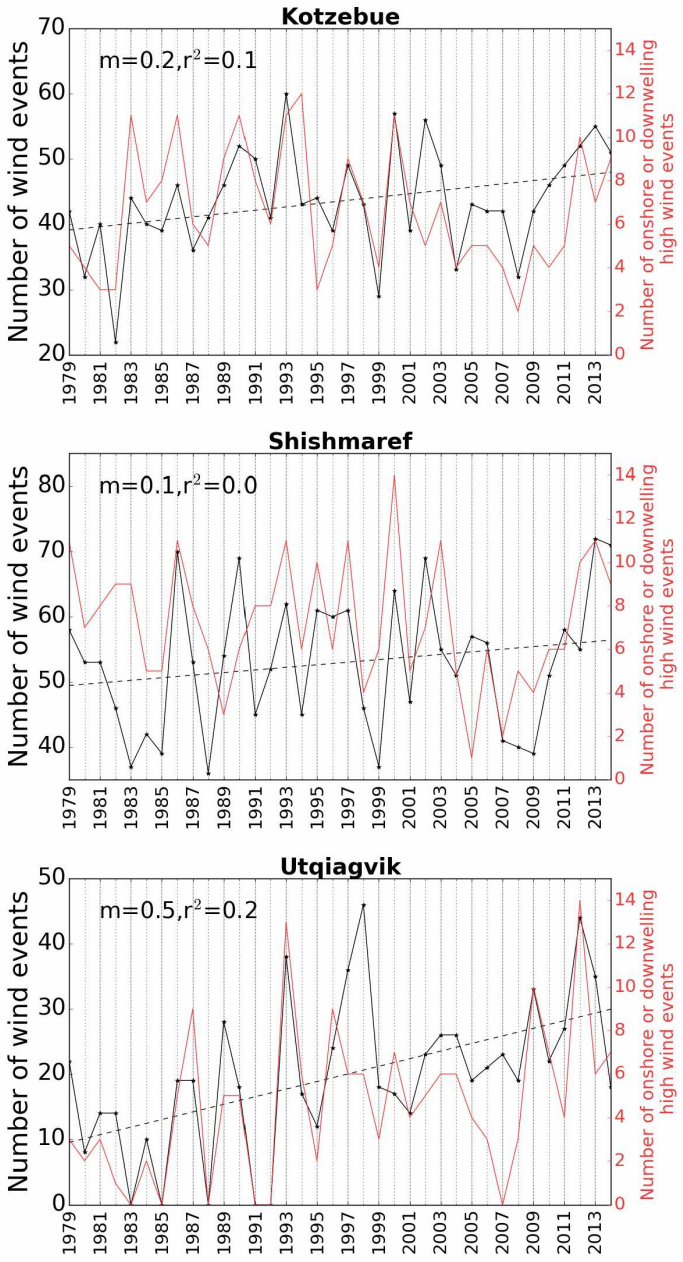

Figure 2.8: The number of wind events capable of causing significant erosion for Kotzebue, Shishmaref and Utqiaġvik. Wind events were defined as being at least 6 hours or longer of sustained winds exceeding 10 m/s including lulls of over 7 m/s shoulder events, as defined in Atkinson (2005). Also shown is the number of these events which have winds in the 90 degree window between the two directions of coming from alongshore (downwelling) and directly onshore toward the community from the ocean, setting up water along the coast. Wind data from WRF-downscaled ERA-Interim, sea ice data from ERA-Interim.

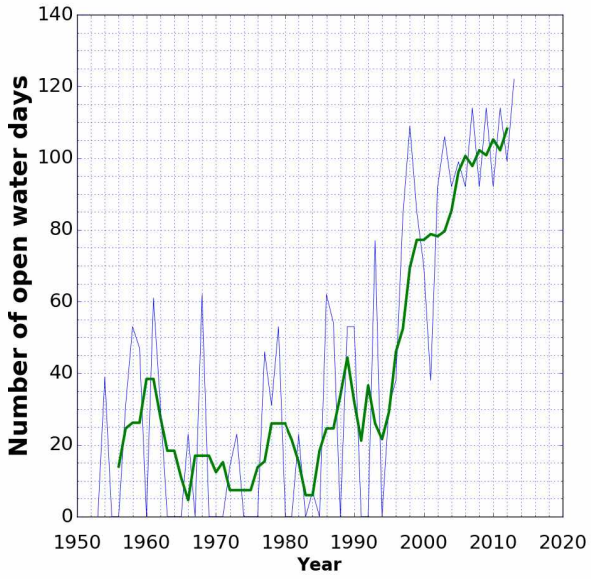

Figure 2.9: Number of open water days at Utqiaġvik, AK has increased substantially since the dataset began in 1953. There has been a marked shift such that after 1992, Utqiaġvik has seen at least some days of open water. Bold green line shows the 5 year running mean of the number of open water days as defined by a 30% sea ice concentration threshold. Data from HSIA.

Table 2.1: Variance of freeze-up and break-up trends

	Trend [days/year]	% variance explained by trend
Freeze-up Kotzebue	0.23	6
Freeze-up Shishmaref	0.60	44
Break-up Kotzebue	-0.10	2
Break-up Shishmaref	-0.34	20

References

Ashjian, C. J., Braund, S. R., Campbell, R. G., George, J. C., Kruse, J., Maslowski, W., Moore, S. E., Nicolson, C. R., Okkonen, S. R., Sherr, B. F., *et al.* (2010). Climate variability, oceanography, bowhead whale distribution, and iñupiat subsistence whaling near barrow, alaska. *Arctic*, pages 179–194.

Atkinson, D. E. (2005). Observed storminess patterns and trends in the circum-arctic coastal regime. *Geo-Marine Letters*, **25**(2-3), 98–109.

Barnhart, K., Overeem, I., and Anderson, R. (2014a). The effect of changing sea ice on the physical vulnerability of arctic coasts. *Cryosphere*, **8**(5).

Barnhart, K. R., Overeem, I., and Anderson, R. S. (2014b). The effect of changing sea ice on the physical vulnerability of Arctic coasts. *The Cryosphere*, **8**(5), 1777–1799.

Berkes, F. and Jolly, D. (2002). Adapting to climate change: social-ecological resilience in a canadian western arctic community. *Conservation Ecology*, **5**(2), 18.

Berman, M. and Kofinas, G. (2004). Hunting for models: grounded and rational choice approaches to analyzing climate effects on subsistence hunting in an Arctic community. *Ecological Economics*, **49**(1), 31–46.

Bieniek, P. A., Bhatt, U. S., Walsh, J. E., Rupp, T. S., Zhang, J., Krieger, J. R., and Lader, R. (2016). Dynamical downscaling of era-interim temperature and precipitation for alaska. *Journal of Applied Meteorology and Climatology*, **55**(3), 635–654.

Callaway, D., Eamer, J., Edwardsen, E., Jack, C., Marcy, S., Olrun, A., Patkotak, M., Rexford, D., and Whiting, A. (1999). Effects of climate change on subsistence communities in alaska. *Assessing the consequences of climate change for Alaska and the Bering Sea Region*, pages 59–73.

Dammann, D. O., Eicken, H., Mahoney, A. R., Meyer, F. J., and Betcher, S. (2018). Assessing sea ice trafficability in a changing arctic. *Arctic*, **71**(1), 59–75.

Dee, D. P., Uppala, S., Simmons, A., Berrisford, P., Poli, P., Kobayashi, S., Andrae, U., Balmaseda, M., Balsamo, G., Bauer, P., *et al.* (2011). The era-interim reanalysis: Configuration and performance of the data assimilation system. *Quarterly Journal of the royal meteorological society*, **137**(656), 553–597.

Department of Commerce, Community, and Economic Development (2017). Alaska Community Coastal Protection Project: Shishmaref Project Page. www.commerce.alaska.gov/web/dcra/PlanningLandManagement/AlaskaCommunityCoastalProtectionProject/Shishmaref.aspx

Druckenmiller, M. L., Citta, J. J., Ferguson, M. C., Clarke, J. T., George, J. C., and Quakenbush, L. (2017). Trends in sea-ice cover within bowhead whale habitats in the pacific arctic. *Deep Sea Research Part II: Topical Studies in Oceanography*.

Eicken, H., Gradinger, R., Gaylord, A., Mahoney, A., Rigor, I., and Melling, H. (2005). Sediment transport by sea ice in the chukchi and beaufort seas: Increasing importance due to changing ice conditions? *Deep Sea Research Part II: Topical Studies in Oceanography*, **52**(24-26), 3281–3302.

Gearheard, S. et al. (2013). *The meaning of ice: People and sea ice in three Arctic communities*. International Polar Institute Press.

Gearheard, S., Matumeak, W., Angutikjuaq, I., Maslanik, J., Huntington, H. P., Leavitt, J., Kagak, D. M., Tigullaraq, G., and Barry, R. G. (2006). It's not that simple: a collaborative comparison of sea ice environments, their uses, observed changes, and adaptations in Barrow, Alaska, USA, and Clyde River, Nunavut, Canada. *AMBIO: A Journal of the Human Environment*, **35**(4), 203–211.

Georgette, S. and Loon, H. (1993). *Subsistence use of fish and wildlife in Kotzebue, a northwest Alaska regional center*. Number 167. Alaska Department of Fish and Game, Division of Subsistence.

Hansen, W. D., Brinkman, T. D., Leonawicz, M., Chapin III, F. S., and Kofinas, G. P. (2013). Changing Daily Wind Speeds on Alaska's North Slope: Implications for Rural Hunting Opportunities. *Arctic*, **66**(4), 448–458.

Huntington, H. P., Gearheard, S., Druckenmiller, M., and Mahoney, A. (2009). Community-based observation programs and indigenous and local sea ice knowledge. *Field techniques for sea ice research*, pages 345–364.

Huntington, H. P., Quakenbush, L. T., and Nelson, M. (2017). Evaluating the effects of climate change on indigenous marine mammal hunting in northern and western alaska using traditional knowledge. *Frontiers in Marine Science*, **4**, 319.

Instanes, A., Anisimov, O., Brigham, L., Goering, D., Khrustalev, L. N., Ladanyi, B., Larsen, J. O., Smith, O., Stevermer, A., Weatherhead, B., and Weller, G. (2005). Chapter 16, Infrastructure: Buildings, Support Systems, and Industrial Facilities. *Arctic Climate Impact Assessment Synthesis Report, Impacts of a Warming Arctic*.

Johnson, M. and Eicken, H. (2016). Estimating arctic sea-ice freeze-up and break-up from the satellite record: A comparison of different approaches in the chukchi and beaufort seas. *Elem Sci Anth*, **4**.

Jones, B. M., Arp, C., Jorgenson, M., Hinkel, K. M., Schmutz, J., and Flint, P. (2009). Increase in the rate and uniformity of coastline erosion in arctic alaska. *Geophysical Research Letters*, **36**(3).

Kapsch, M.-L., Eicken, H., and Robards, M. (2010). Sea ice distribution and ice use by indigenous walrus hunters on st. lawrence island, alaska. In *SIKU: Knowing Our Ice*, pages 115–144. Springer.

Kovacs, A. and Sodhi, D. S. (1980). Shore ice pile-up and ride-up: Field observations, models, theoretical analyses. *Cold Regions Science and Technology*, **2**, 210–288.

Kovacs, K. M., Lydersen, C., Overland, J. E., and Moore, S. E. (2011). Impacts of changing sea-ice conditions on arctic marine mammals. *Marine Biodiversity*, **41**(1), 181–194.

Krupnik, I. and Jolly, D. (2002). *The Earth Is Faster Now: Indigenous Observations of Arctic Environmental Change. Frontiers in Polar Social Science*. ERIC.

Laidler, G. J., Ford, J. D., Gough, W. A., Ikummaq, T., Gagnon, A. S., Kowal, S., Qrunnut, K., and Irngaut, C. (2009). Travelling and hunting in a changing arctic: assessing inuit vulnerability to sea ice change in igloolik, nunavut. *Climatic Change*, **94**(3-4), 363–397.

Light, B., Eicken, H., Maykut, G., and Grenfell, T. (1998). The effect of included participates on the spectral albedo of sea ice. *Journal of Geophysical Research: Oceans*, **103**(C12), 27739–27752.

Mahoney, A. R., Eicken, H., Gaylord, A. G., and Gens, R. (2014). Landfast sea ice extent in the chukchi and beaufort seas: The annual cycle and decadal variability. *Cold Regions Science and Technology*, **103**, 41–56.

Marino, E. (2012). The long history of environmental migration: Assessing vulnerability construction and obstacles to successful relocation in shishmaref, alaska. *Global environmental change*, **22**(2), 374–381.

Moore, S. and Huntington, H. (2008). Arctic marine mammals and climate change: impacts and resilience. *Ecological Applications*.

NANA Regional Corporation (2016). Kotzebue Village Profile. [http://nana.com/regional/about-us/overview-of-region/kotzebue/.

Norton, D. W. and Gaylord, A. G. (2004). Drift velocities of ice floes in alaska's northern chukchi sea flaw zone: Determinants of success by spring subsistence whalers in 2000 and 2001. *Arctic*, pages 347–362.

Overeem, I., Anderson, R. S., Wobus, C. W., Clow, G. D., Urban, F. E., and Matell, N. (2011). Sea ice loss enhances wave action at the Arctic coast. *GRL*, **38**(17).

Parkinson, C. L. (2014). Spatially mapped reductions in the length of the arctic sea ice season. *Geophysical research letters*, **41**(12), 4316–4322.

Parkinson, C. L. and Comiso, J. C. (2013). On the 2012 record low arctic sea ice cover: Combined impact of preconditioning and an august storm. *Geophysical Research Letters*, **40**(7), 1356–1361.

Serreze, M. C., Crawford, A. D., Stroeve, J. C., Barrett, A. P., and Woodgate, R. A. (2016). Variability, trends, and predictability of seasonal sea ice retreat and advance in the chukchi sea. *Journal of Geophysical Research: Oceans*, **121**(10), 7308–7325.

Smith, L. C. and Stephenson, S. R. (2013). New trans-arctic shipping routes navigable by midcentury. *Proceedings of the National Academy of Sciences*, **110**(13), E1191–E1195.

Solomon, S. M., Forbes, D., and Kierstead, B. (1994). *Coastal impacts of climate change: Beaufort Sea erosion study*. Geological Survey of Canada Ottawa.

Thomson, J. and Rogers, W. E. (2014). Swell and sea in the emerging arctic ocean. *Geophysical Research Letters*, **41**(9), 3136–3140.

Walsh, J. E., Fetterer, F., Scott Stewart, J., and Chapman, W. L. (2017). A database for depicting arctic sea ice variations back to 1850. *Geographical Review*, **107**(1), 89–107.

Zhang, X. and Zhang, J. (2001). Heat and freshwater budgets and pathways in the arctic mediterranean in a coupled ocean/sea-ice model. *Journal of oceanography*, **57**(2), 207–234.

Chapter 3

Increasing wind energy input over a lengthened open water season influences freeze-up timing in Alaska waters

Rolph, R. J., Mahoney A. R., Walsh J., Winsor, P., Simmons, H. (2018, *in prep.*). Increasing wind energy input over a lengthened open water season influences freeze-up timing in Alaska waters. *Journal of Geophysical Research: Atmospheres.*

3.1 Abstract

An extended Arctic open water season, especially as freeze-up moves into the fall storm season, leaves more time for wind stress to act on open water. This impacts air-sea momentum transfer and heat exchange which are essential to distribute heat throughout the global ocean. To assess how the wind energy input is changing in conjunction with recent sea ice loss, we have evaluated multi-decadal trends in the Bering, Chukchi, and southern Beaufort Seas from 1979-2014 for cumulative wind energy input over open water and wind speeds 1 month prior to freeze-up. We have also provided a climatology of the weekly-averaged wind speeds for Alaska waters. Average wind speed during the open water season and in the month before freeze-up has increased in the Chukchi and southern Beaufort Seas due to delayed freeze-up into the fall storm season. Throughout the Chukchi and southern Beaufort Seas, the date of freeze-up is positively correlated with the cumulative wind energy input into open water beforehand, indicating that storms tend to delay freeze-up there. However, the correlation increases with the length of the wind integration period and is near zero for periods shorter than approximately 7 days, indicating individual storms immediately before freeze-up have little effect. Near the southern extent of sea ice in the Bering Sea, the correlation is negative, an indicator that storms promote the arrival of ice in this region. Mechanisms to explain why higher wind speeds tend to delay freeze-up in the Chukchi Sea and promote freeze-up in the Bering Sea are explored through the use of case studies.

3.2 Introduction

Under a declining Arctic sea ice cover, the upper ocean has longer exposure to the atmosphere, which can result in increased wind waves and upper ocean mixing as freeze-up is delayed into the fall storm season. When parametrizing carbon and heat fluxes within the atmospheric boundary layer over the ocean, the impact of the surface ocean on the atmosphere must also be considered because the ocean exhibits a drag on surface winds moving across the water. Surface drag changes depending on the form of the ocean surface, whether it is covered entirely in sea ice, open water, or is a marginal ice zone (partial ice cover). Wind-waves, created by wind stress on the upper ocean, change surface drag based on wave height (*Taylor and Yelland*, 2001). Hence, a longer open water season will influence energy transfer from the atmosphere to the ocean. We aim to quantify upper-ocean wind energy input for the lengthened open water seasons observed in the Bering, Chukchi, and southern Beaufort Seas. Wind waves are considered a significant Arctic shipping hazard (*Aksenov et al.*, 2017) and threat to coastal infrastructure, and have been documented to increase shoreline erosion (*Overeem et al.*, 2011). We have decided to perform analysis during the open water season instead of times of partial sea ice cover, because the wind-wave hazard is more prevalent in this season.

Understanding the controlling factors which determine freeze-up timing can give insight about how the strength of air-sea feedbacks might change in the future. Once these factors have been identified, the relative dominance of each factor can vary regionally, such as differences in the importance of heat inflow in different parts of the Arctic Ocean. *Serreze et al.* (2016) investigated

factors that control freeze-up timing in the Chukchi Sea, which include Bering Strait heat inflow, radiation fluxes, temperature, and wind. Bering Strait inflow was found to explain 67% of the sea ice advance date variance in the Chukchi Sea. The magnitude of impacts of Bering Strait inflow, heat fluxes and temperature are all ultimately connected by winds. This is due to the Bering Strait inflow being connected with large-scale Pacific-Atlantic atmospheric pressure patterns. Also, there is a dependence of net air-sea heat flux on the strength of the air-sea temperature gradient and amount of wind-driven mixing.

In addition to quantifying the change in wind energy input over open water for the different seas in the Alaska subdomain, we evaluate the correlation between the wind energy input and freeze-up timing over different integration periods in order to determine when winds matter most for freeze-up timing. This paper aims to answer the main research questions of how the Bering, Chukchi, and southern Beaufort Seas have changed over the satellite era in: open water season duration, wind energy input over open water, and average wind speed prior to freeze-up. We also evaluate causes for differences in the relationship of wind speed and freeze-up timing in the Chukchi and Bering Seas.

3.3 Data and Methods

3.3.1 Selection of subdomains and definition of open water

The Chukchi and southern Beaufort Seas lie on the west and north of Alaska in the Arctic Ocean. These seas are important for goods and fuel delivery by barge, animal migration, and have exhibited some of the fastest changes in sea ice extent in recent years (*Stammerjohn et al.*, 2012). In the domain of our available dataset, a well-defined ice edge in the northern Chukchi Sea in late fall (Figure 3.1a) was apparent for several of the years observed. Since we have chosen to identify trends in the open water season, this spatial pattern also shows how the sea ice boundary provides a natural subdomain boundary between the Beaufort and Chukchi Seas (subdomain boundaries are given in Figure 3.1a). The Bering Sea subdomain was selected within the extent of the domain of the full available dataset. These domains were also separated because they each have water masses with different properties and circulation. The winds and sea ice concentration data in these subdomains were taken from the WRF-downscaled ERA-Interim product (*Bieniek et al.*, 2016) as described in Section 3.3.2. To investigate the trends in open water duration for each sea, we counted the number of days for each grid cell in each subdomain when the sea ice concentration was below the threshold of 15%. These values were then averaged over the number of grid cells in each subdomain to obtain the average open water period for each sea. Linear trends in open water duration (days/year) were found for each subdomain.

3.3.2 WRF-downscaled ERA-Interim data and wind speed climatology

Using an Advanced Research version of the Weather Research and Forecasting (WRF) regional model, the European Centre for Medium-Range Weather Forecasts interim reanalysis (ERA-Interim) dataset (*Dee et al.*, 2011) has been dynamically downscaled (*Bieniek et al.*, 2016). The downscaled

dataset covers the time period of 1979-2014 and has an hourly resolution (daily for sea ice) with 20 km spatial resolution. The parent ERA-Interim dataset has a 0.75 degree (about 83 km) spatial resolution and 6 hourly temporal resolution. ERA-Interim prescribes sea ice as a boundary condition in the atmospheric model, and is assimilated with several different SST and SIC products. The downscaled dataset was developed to improve precipitation and temperature representation around Alaska's varying terrain and complex coastline, and to inform various stakeholders with higher-resolution climate and weather information. The WRF regional model uses a thermodynamic sea ice model (*Zhang and Zhang*, 2001), coupled with the Noah land surface model used within the WRF model to accurately simulate the thermal conditions over sea ice. To derive a climatology of wind speed, we calculated mean wind speeds on a weekly basis from hourly data for the period of 1979-2014 for every grid cell in the study domain. These climatologies allow us to determine the timing of the storm season, the peak of which we define by finding the week with the highest average wind speed.

3.3.3 Calculating wind energy input over open water and wind speeds prior to freeze-up

The wind energy input over open water was calculated for each hourly timestep in each grid cell of the selected subdomains. The wind energy for those timesteps was calculated using the equation of *Denman and Miyake* (1973) and multiplied by 1 hour to approximate the integration of wind energy over each timestep.

$$\frac{\delta E}{\delta t} = \rho m C_d u^3 \tag{3.1}$$

where $\rho = 1.2\frac{kg}{m^2}$ is air density, m = 10^{-3} is an efficiency factor, and $C_d = 10^{-3}$ is a drag coefficient, u is wind speed at 10 m above sea level. A similar technique was also applied by *Hauri et al.* (2013).

The cumulative wind energy input was found by summing the wind energy input over the open water timesteps for each grid cell. The cumulative wind energy input over open water for all grid cells in each subdomain was averaged to obtain one value per calendar year for each sea. Linear trends in the annual cumulative wind energy input over open water (J/m^2 per year) were also calculated for each grid cell to better observe variation within each subdomain, and insignificant trends (p-value > 0.05) greyed out.

The average wind speed in the time period before freeze-up was calculated in a similar way. Freeze-up is defined as the day of 15% sea ice cover before the longest ice-covered period of the season. In some cases, a late freeze-up may be early in the calendar year because it corresponds to the end of the open water season of the previous year. If freeze-up was early in the calendar year, wind data from the previous year was used to fill the wind timeseries for the specified time period before freeze-up. The wind speeds in the time window at 31 days prior to freeze-up for each year were averaged into one value for each grid cell. Then, this average value for each grid cell was used to calculate the mean of the entire subdomain. One value was found for each sea for each year and presented in a yearly timeseries.

3.3.4 Correlation between wind energy input and freeze-up timing

To investigate when upper-ocean wind-driven mixing might be most important in determining freeze-up timing, correlation coefficients were calculated for each grid cell in the 35 year timeseries (1980-2014) over the entire domain of the dataset. For each year, the cumulative wind energy input in a time integration period (from 1 through 93 days) prior to freeze-up was calculated for each grid cell. 93 days was used to examine the impact of winds before freeze-up on a seasonal timescale. This means a total of 93 values of cumulative wind energy input were found for each grid cell for each year, with each of the 93 values representing the total wind energy input for a different length of time integration period prior to freeze-up. The yearly timeseries of each respective cumulative wind energy value of the corresponding time integration period was correlated with the yearly timeseries of freeze-up timing for each grid cell. For example, the yearly timeseries of the cumulative wind energy input for a grid cell in the 93 day time integration period prior to that grid cell's freeze-up timing was correlated with the yearly timeseries of that grid cell's freeze-up timing. We then found the time window prior to freeze-up that revealed the highest magnitude correlation coefficient between cumulative wind energy input and freeze-up timing.

The areas with grid cells that had less than 80% of the years with a defined freeze-up date (those cells which had no open water period or only open water for the full calendar year) were excluded from all correlation calculations in order to reduce bias from a low number of data points. In some cases (in the northerly region of the domain) the open water season length was shorter than 93 days. We needed to reduce bias when calculating correlation values with wind energy input over open water for time periods longer than the open water season length. To do this, if more than 80% of the years at a grid cell did not have an open water season length of at least the time integration period used in the correlation before freeze-up, the last correlation value which met this threshold was used. For those grid cells where this was applied, it results in shorter time windows before freeze-up possible to have a maximum correlation between wind energy and freeze-up timing. Some grid cells also had an equal maximum correlation value for different time periods, and when this happened, the longest time period was used. We have marked which grid cells these are in the Results section.

3.3.5 Case studies

Results from the correlation values described above differed significantly between the Chukchi and Bering Seas, which motivated the use of case studies in each of these locations to explain the underlying mechanisms in both of these regions. To explain the contrasting positive and negative correlation between wind speeds and freeze-up timing between the Chukchi and Bering Seas, two locations were selected in each, and are given in Figure 3.5a. Point A (69.3 N, -170.3 W) was selected because it is in the middle of the shelf and squarely in the Chukchi Sea. The location A also had an open water duration of at least 93 days for at least 80% of the years from 1979-2014. Point B was selected to represent the Bering Sea (58.2 N, -168.5 W) because it has a significant

negative correlation value. It is also along the seasonal maximum sea ice edge, which is very different than the more consistent seasonal ice regime of the Chukchi Sea. The timeseries which produce the correlation values at Points A and B for the 93 day time period are also given.

Two years were selected for both the Chukchi and Bering Seas, totalling four separate case studies, to investigate possible causes of the contrasting correlation values. Given the positive correlation in the Chukchi Sea, a year with a late freeze-up and high cumulative wind energy from the detrended timeseries was selected (2007). Another year was selected, with a relatively early freeze-up and low cumulative wind energy (2008). In contrast, given the negative correlation in the Bering Sea, a year with an early freeze-up and high cumulative wind energy was selected (2002), and a second year with a late freeze-up and low wind energy (2005). Daily averaged wind speeds, directions, sea ice concentration, as well as hourly 2 m air temperature are given 3 months prior to freeze-up for both case study years in the Chukchi sea location (Point A). Given the shorter timescales of maximum correlation between winds and freeze-up timing in the Bering Sea, the same variables in the 1 month instead of 3 months prior to freeze-up are analyzed.

3.4 Results

3.4.1 Increasing wind speeds and duration of open water before freeze-up

The open water seasons of both the Chukchi and southern Beaufort Seas have increased (Figure 3.1a,c,d), along with the mean annual cumulative wind energy input into open water in these regions. Over the 35-year time period, the open water seasons in both regions grew by 53% and 279%, respectively, while the wind energy input over this season increased by 49% and 152%, respectively. These trends show significant p-values. In the Bering Sea domain examined (Figure 3.1a), the open water season has increased because of regional increases in the number of days with sea ice cover in Bristol Bay. The decrease of the open water season there is -8%, and the wind energy input into open water shows an insignificant decreasing trend of 14%.

Both the Chukchi Sea and southern Beaufort Sea regions show trends toward significant increased windspeeds in the month prior to freeze-up during the 35-year study period. In the southern Beaufort Sea, the trend is almost 2 times that found in the Chukchi Sea (Figure 3.2). When a linear trend line is fitted, the southern Beaufort Sea shows a rate of increase of about 0.4 m/s wind speed before freeze-up per decade, from about 5.7 m/s to about 7.0 m/s over the 36 year time period from 1979-2014. The Chukchi Sea shows an increase from about 7.4 m/s near the beginning of the dataset to about 8.0 m/s towards the end of the dataset, giving a rate of increase in wind speed the month before freeze-up of approximately 0.2 m/s per decade (Figure 3.2). The Bering Sea shows a small but significant decrease in the average wind speeds in the month prior to freeze-up (Figure 3.2c). In general, the wind speeds are larger in the month prior to freeze-up in the Bering Sea than they are in either the Chukchi or southern Beaufort Seas.

We did not find a significant change from 1979-2014 in the wind climatologies between the three study domains (Figure 3.3). There are clear seasonalities of windier seasons in winter and fall, which are enhanced in the more southern domains. For example, the Bering Sea shows more

variation with calmer winds in mid-summer and higher winds in winter and fall (Figure 3.3c) than the southern Beaufort Sea (Figure 3.3a).

3.4.2 Maps of correlation between wind energy input and freeze-up timing

The trend of annual cumulative wind energy input into the upper ocean (Figure 3.4a) agrees with trends observed in changes of sea ice cover (Figure 3.4b). The maximum correlation values between cumulative wind input prior to freeze-up and the date of freeze-up are positive throughout our study region, except at the southernmost extent of the ice pack in the Bering Sea, where there is a negative correlation (Figure 3.4c). As we narrow the time integration period such that it begins closer to the timing of freeze-up (e.g. 1 day), low correlation values exist for all regions. The time periods before freeze-up with the highest correlation values are longer in the Chukchi Sea and southern Beaufort Sea (2-3 months) than they are in the northeastern Bering Sea (Figure 3.4d). The correlation values of cumulative wind energy input during the 93 days prior to freeze-up and freeze-up timing showed a strong positive correlation in the Chukchi and strong negative correlations in the Bering Sea. Results of the four case studies in these regions (Points A and B for the Chukchi and Bering Seas, respectively in Figure 3.5a) are discussed in the following two sections.

3.4.3 Results of case studies: Chukchi Sea

Cumulative wind energy input in the month prior to freeze-up in the Chukchi Sea has low correlation values with freeze-up timing, with increasing values on longer timescales (Figure 3.6a). At the location on the Chukchi Shelf (point A given in Figure 3.5a) there was a late freeze-up in 2007 (December 15) compared to the early freeze-up occurring in 2008 (November 19). The winds in the three months prior to freeze-up in 2007 were stronger than the winds in the three months prior to freeze-up in the year 2008, but both had wind components coming from the dominant northeasterly wind direction (Figure 3.7a and b). Not only were they stronger in 2007, but the winds also did not come from between the northwest and southwest as often. In 2008, this was not the case, and some of the wind before ice cover occurred was northwesterly and southwesterly.

The 2 m air temperatures between the two years showed relatively similar magnitudes in the three months prior to freeze-up (Figures 3.7c and d). However, 2008 showed a consistent drop in 2 m air temperature, from above 5°C to approximately -5°C at the time of freeze-up. This is a more steady drop in 2 m air temperature than compared to 2007, which oscillated around -5°C from 42 days to a week before freeze-up. Not only did 2008 show a more consistent trend in 2 m air temperature, 2008 also showed a more consistent period of open water at Point A in the Chukchi Sea before freeze-up at that location. In 2007, there was about a 20% sea ice cover about a week before the start of the longest ice-covered period of the 2007 season, when in 2008 there was uninterrupted open water for the full 3 months prior to the ice-covered period (compare blue lines in Figures 3.7c and d).

3.4.4 Results of case studies: Bering Sea

In the location selected for the Bering Sea (Point B in Figure 3.5a), significant differences in the wind directions before freeze-up occurred between the late (April 7, 2005) and early (Jan 19, 2002) freeze-up seasons. In the month prior to freeze-up, the late freeze-up season had significantly less winds coming from northerly directions in the month prior to freeze-up (Figure 3.8a) than occurred in the year with an early freeze-up (Figure 3.8b). The early freeze-up season lacked strong winds from the southwest (Figure 3.8b), which typically bring in warm air. The early freeze-up season also had more sharp drops in air temperature than the later freeze-up season in the days leading up to each corresponding longest ice-covered season (compare red lines in Figures 3.8c and d). In the month prior to freeze-up in 2002, there was a drop in air temperature and increase in northwesterly and northeasterly winds, with a corresponding increase in sea ice cover. This resulted in a 25-day period with ice concentration greater than 15%, as defined in Section 3.3.3 (see blue line in Figure 3.8d). Such 'false freeze-ups' are not uncommon in the reanalysis record, particularly in the Bering Sea (not shown).

3.5 Discussion

The wind climatology gradient for the fall freeze-up season is roughly +0.25 m/s per week for the Bering Sea and +0.2 m/s per week for the Chukchi and southern Beaufort Seas (Figure 3.3). If we assume the rate of the delay of freeze-up is equivalent to half of the rate of increase in the number of open water days (Figure 3.1), we obtain a change in the timing of freeze-up by roughly -0.43, +1.0, and +1.4 week per decade for the Bering, Chukchi, and southern Beaufort Seas respectively. Multiplying the wind speed climatology gradient by the change in freeze-up timing, we should therefore expect a change in wind speed in the period before freeze-up by -0.01, +0.02, and +0.03 m/s per year for the Bering, Chukchi, and southern Beaufort Seas respectively. Since the wind climatology does not show significant changes between 1979-2014 (compare Figures 3.3b and c), the observed increases in wind speeds in the period prior to freeze-up is primarily a result of the freeze-up season moving further into the fall storm season (Figure 3.2). As long as the freeze-up season is delayed during a period of increasing climatological wind speeds (see fall season in Figure 3.3), we can expect the wind speeds in the period prior to freeze-up to also increase.

Storms can potentially promote or delay freeze-up by different mechanisms, three of which we will discuss here. We have found that the greatest positive correlation of wind energy input and freeze-up timing occurs 2-3 months prior to freeze-up in the Chukchi and southern Beaufort seas. So overall, just a few storms prior to freeze-up do not have a significant impact on freeze-up timing, and storms do not cause an earlier freeze-up. We apply these results to the mechanisms described below and can eliminate which mechanisms are less dominant in controlling freeze-up timing in the Chukchi and southern Beaufort seas.

The first mechanism involves storms strong enough to break the halocline and entrain warmer water from below into the mixed layer, as observed in *Yang et al.* (2004). However, as observed in *Long and Perrie* (2012), storms in the coastal southern Beaufort can also cool the mixed layer by

up to 2°C if they entrain cooler water from below. Cooling of the sea surface by as much as 4°C in the wake of hurricanes has also been found in the mid-latitudes, followed by subsequent sea surface warming (*Price et al.*, 2008). This mechanism of sea surface cooling after storm passage in the mid-latitudes is due to the upper ocean of mid-latitudes entraining cooler water at depth. Depending on what relative temperature water is entrained into the mixed layer, freeze-up would be delayed due to the excess heat which must be lost in the mixed layer, or hastened because less heat must be lost to reach freezing temperature. Our results suggest that entrainment of cooler water from below by storms in the Chukchi and southern Beaufort is not a dominant mechanism to change the timing of freeze-up.

A second mechanism by which storms influence freeze-up timing has to do with their mechanical mixing of the upper ocean. Not only do storms change the magnitude of the sensible heat flux by changing the air-sea temperature gradient, but storms cool the upper ocean by increasing sensible heat flux due to increased upper ocean mixing. This increased mechanical mixing increases the relative surface area of the ocean exposed to the cooler atmosphere, resulting in more efficient heat release. This mechanism suggests storms hasten freeze-up, but only if the ocean is warmer than the atmosphere (as is the case during freeze-up). If the air-sea temperature gradient is low, then increased mechanical mixing will not have much of an effect. Although this is a plausible mechanism by storms to hasten freeze-up, our results show this is not a dominant mechanism to control freeze-up timing in the Chukchi and southern Beaufort because we have found a positive correlation between cumulative wind energy input and later freeze-up timing.

Freeze-up does not need to be defined from purely thermodynamic processes. A third mechanism of storms' impact on freeze-up timing is wind-driven ice advection into an area. Ice advection as a cause of freeze-up acts on shorter timescales (order of days) than the time it takes for heat in the water column accumulated over the summer to be lost to the atmosphere (from days to months). Ice advection is particularly important in determining Bering Sea freeze-up timing (*Overland and Pease*, 1982). The time integration period with the highest correlation of wind energy input to freeze-up timing in the Bering Sea is shorter (order of 20 days) than the Chukchi and southern Beaufort (2-3 months, Figure 3.4d). Given these different timescales, our results also support ice advection by storms as a dominant factor in controlling freeze-up timing in the Bering Sea, but show it is not generally a dominant factor in the Chukchi or southern Beaufort. This is discussed in subsections 3.5.1 and 3.5.2 in more detail.

3.5.1 Case studies: Role of winds in changing freeze-up timing of the Chukchi Sea

The dominant northeasterly wind direction in the Chukchi Sea is evident in both years selected for the case studies, but it is more pronounced during the windier season before the late freeze-up in 2007 (compare Figures 3.7a and b). Strong northeasterly winds tend to promote upwelling of warm Atlantic waters. Lower halocline waters of the western Arctic (salinity > 34 psu and temperatures about 1°C) can upwell onto the Chukchi shelf and subsequently mix with Pacific waters (*Woodgate et al.*, 2005). Although warm and salty Atlantic water has been shown to upwell

onto the Chukchi Borderland-Mendeleeve Ridge region (*Woodgate et al.*, 2005), it has also been observed well onto the Chukchi shelf (*Bourke and Paquette*, 1976). Upwelling is more frequent in fall, and the resulting salt and heat fluxes can be significant onto the Chukchi shelf (*Aagaard and Roach*, 1990). Mixing of the relatively warm and salty waters onto the shelf in the months prior to freeze-up would suggest ice formation to be delayed there. Since the location of the case study is squarely in the middle of the shelf (Figure 3.5a), this could be one of the mechanisms to explain the later freeze-up timing of the higher wind seasons prior to freeze-up. The timescales of this upwelling and associated mixing roughly match those timescales with the highest correlations of freeze-up timing and cumulative wind energy input ($>$ 80 days in Figure 3.6a). This suggests that seasonal timescales of increased wind energy input into the upper ocean in the Chukchi Sea are more important to determine the timing of freeze-up than shorter timescales. Those processes associated with shorter timescales (e.g. ice advection) reach a maximum faster (starting at roughly 1 week) in the Bering Sea (Figure 3.5b).

Not only do strong northeasterly winds promote upwelling, but they can also advect cold air from the north into the region. This was the case in the three months prior to freeze-up in 2007, which reached a cooler 2 m air temperature at an average -5°C roughly 42 days prior to freeze-up until freeze-up timing. This is compared to an average temperature of -5°C not being reached until roughly 1 week before the earlier freeze-up in 2008, which had much lower levels of wind advection (compare red lines in Figure 3.7c and d). Freeze-up took longer to occur in 2007 despite the persistent cooler air temperatures before freeze-up compared with 2008. Given the more persistent freezing air temperatures during that later freeze-up season of 2007, the warmer water preconditioning in 2007 had more of an influence on the timing of freeze-up compared with surface air temperatures.

3.5.2 Case studies: Role of winds in changing freeze-up timing of the Bering Sea

Atmospheric forcing effects in the Bering Sea largely determine the circulation and oceanographic properties in the Bering Sea. This is due to flow over the shelf tending to be slow and also to the physical separation of the Bering and Gulf of Alaska by the Alaska Peninsula (*Pease*, 1980). The wind directions in the two case studies in the month prior to freeze-up at the location chosen in the Bering Sea (Point B in Figure 3.5a) varied significantly between 2002 (early freeze-up season) and 2005 (late freeze-up season). By comparing the progression of the sea ice edge during the freeze-up seasons of these two years, we find advective processes of both air and sea ice are important for the timing of freeze-up in both of these seasons. This can explain why the shorter timescales (advective timescales) have the highest correlation between cumulative wind energy input and freeze-up timing for a large part of the Bering Sea (see cooler colors in the Bering Sea in Figure 3.4d).

In 2005, the sea ice edge loitered close to Point B in the Bering Sea for more than 1 month prior to the freeze-up of Point B. This loitering or slow advance of the sea ice edge is caused by the more balanced southwesterly and northwesterly winds in the one month prior to freeze-up, as well as

a relatively stable air temperature (Figure 3.8 a and c). In 2002, the sea ice edge progressed more rapidly, starting near the Bering Strait one month prior to freeze-up and in under 4 weeks actually surpassing Point B before receding again northwards (not shown). The rapid advance of the sea ice edge was caused by sea ice and cold air advection from strong northeasterly and northerly winds in the month prior to freeze-up (Figure 3.8b). After advancing southward of Point B in the Bering Sea, the ice edge then retreated due to very strong (from 13 to 16 m/s) warm, southeasterly winds which both increased the 2 m air temperature (see rapid increase in 2 m air temperature at around 10 days, red line in Figure 3.8d) and compressed the ice pack northwards. Cold easterly winds then caused the ice edge to advance for the final time of the 2001-2002 season to Point B to start the longest ice covered season there.

3.5.3 Changes in wind energy input prior to freeze-up and relationship with timing of freeze-up

Winds are shown to be of significant consequence for the timing of freeze-up in the Chukchi Sea, with the opposite relation in the Bering Sea. Given the predominant northeasterly wind directions in the Chukchi Sea and southern Beaufort Sea, and the fact that strong winds coming from this direction tend to promote upwelling of warm, salty, Atlantic water (*Woodgate et al.*, 2005), it makes sense that higher wind speeds are more highly correlated with a later freeze-up at these more northerly regions. As well, the longer timescales associated with mixing of upwelled water toward the Chukchi Sea shelf can also help explain why the highest correlations are happening over longer timescales (order of months) prior to freeze-up (Figure 3.4d).

Ocean-atmosphere interactions specifically prior to freeze-up are also likely to be enhanced in recent years in the Beaufort Sea rather than in the Chukchi Sea. We expect a faster rate of change in the increase of significant wave height and turbulent heat flux exchange in the southern Beaufort Sea compared to the Chukchi Sea. Annual differences in the rate of change of cumulative wind energy transfer over the entire open water period from the atmosphere to the ocean between the Chukchi and southern Beaufort are comparable to those in the months before freeze-up (compare slope of red lines in Figures 3.1c and d, and warm colored values in 3.4a).

During the freeze-up season, a positive ocean heat flux can retard or reverse the freezing process when stratification is relatively weak. Warm water can be brought from depth to the surface by winds strong enough to break the halocline (*Yang et al.*, 2004). Not only is stratification weak during the freeze-up season, but fall storms and a northward moving storm track also contribute to a deeper mixed layer. In this study we have mapped the linear trends in annual cumulative wind energy over open water, which unsurprisingly correlates well with the spatial patterns in linear trends of the change in open water duration (Figure 3.4a and b).

Examining winds in the time integration period 3 months prior to freeze-up timing, the correlation between wind energy input and freeze-up timing is highest in the northern Chukchi and southern Beaufort Sea, and lowest in the Bering Strait region (Figure 3.4c). So for the time period 3 months prior to freeze-up, these results suggest that in the Bering Strait region, other factors, such

as Bering Strait heat inflow (as shown by *Serreze et al.* (2016)) are more dominant in controlling the timing of freeze-up than wind-driven mixing. Indeed, Bering Strait heat inflow has been found to explain most of the variance of freeze-up timing in the Bering Strait and southern Chukchi region over monthly timescales (July-September) (*Serreze et al.*, 2016).

In essence, a region with a longer time integration window associated with the highest correlation suggests a single storm has less of an impact on the timing of freeze-up in that region. In other regions showing a maximum correlation at shorter time integration periods, single storms statistically will have more of an influence on freeze-up timing. We found that the Chukchi Sea has a maximum correlation in a time integration period longer than the Bering Sea. This suggests that a single storm is less statistically related to the timing of freeze-up in the Chukchi than in the Bering Sea. Seasonal evaluation of vertical heat fluxes and horizontal advective processes in the ocean and surface winds in the time period prior to freeze-up is a logical next step.

3.6 Conclusions

We have shown due to delayed freeze-up into the windier fall season, there are now greater wind speeds in the period prior to freeze-up. This leads to increased wind energy input over open water, upper-ocean mixing, and advection. In the Chukchi Sea, late freeze-up years are associated with high winds from the northeast, which can cause upwelling onto the Shelf. In the Bering Sea, early freeze-up is associated with high winds from the north, advecting ice and cold air into the region. Since the windier seasons in the Chukchi Sea and southern Beaufort Sea are associated with upwelling of heat, that suggests winds promote delayed freeze-up, resulting in a potential positive feedback mechanism. But, the correlation analysis suggests that individual storms do not have a short term impact on freeze-up itself. It is the windier season which has more influence on the timing of freeze-up. Processes such as upwelling and subsequent mixing and replacement of Chukchi Shelf waters acting on longer timescales are the more dominant control of freeze-up of the Chukchi Sea.

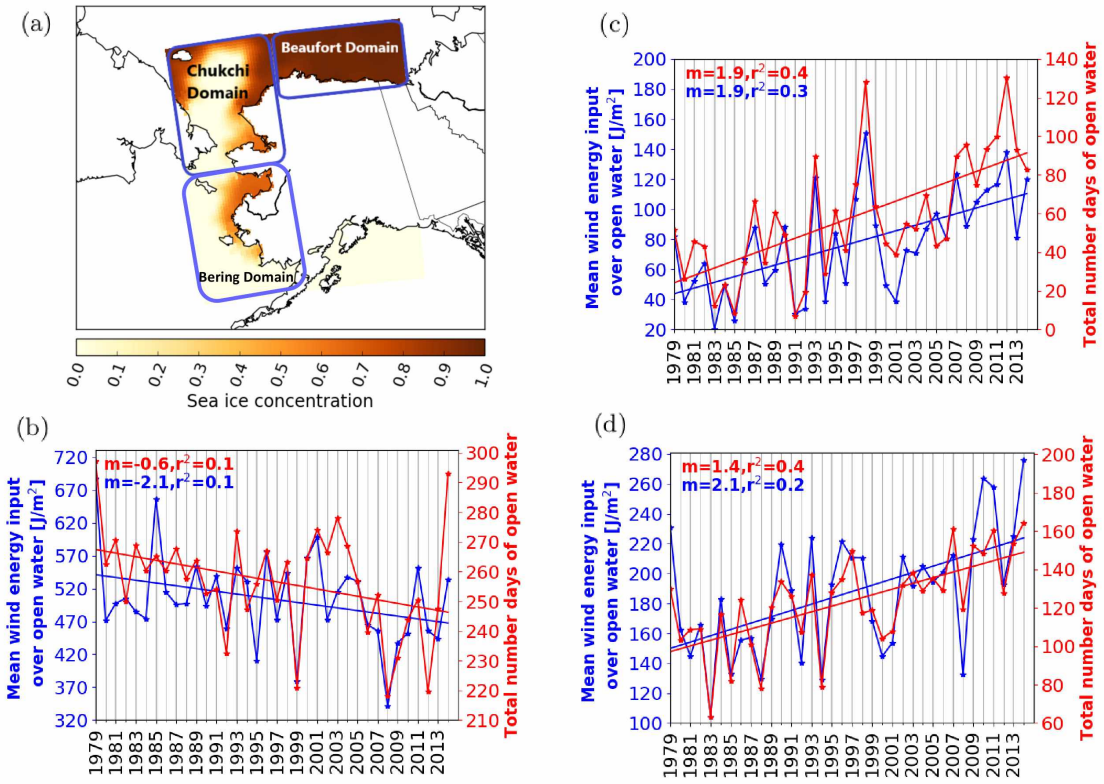

Figure 3.1: (a) Map of the southern Beaufort, Chukchi, and Bering Sea subdomains selected for analysis of increased wind energy input over the lengthened open water season. Sea ice concentrations are from early November 2011. Cumulative wind energy input over open water and open water duration for the time period of 1979-2014 for (b) the Bering Sea (c) southern Beaufort Sea and (d) Chukchi Sea.

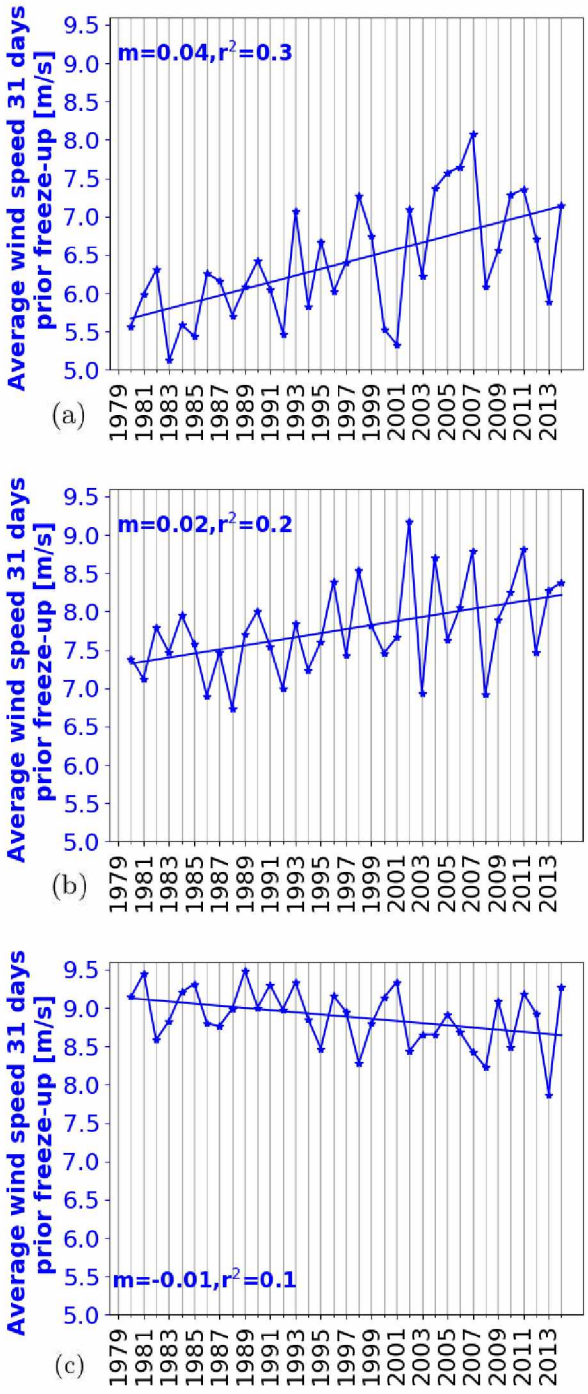

Figure 3.2: Average wind speeds in the month prior to freeze-up for the (a) southern Beaufort (b) Chukchi and (c) Bering Seas.

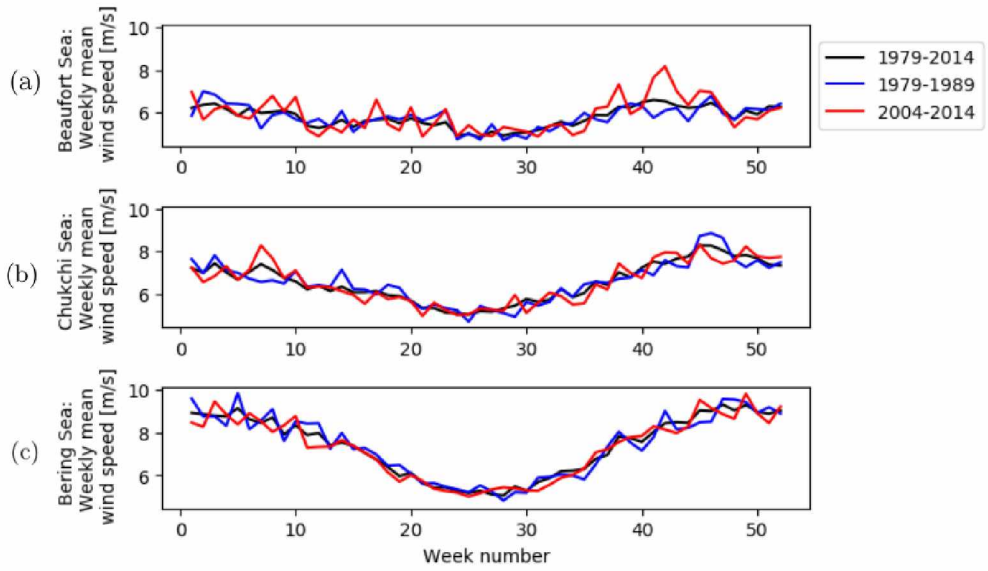

Figure 3.3: Weekly-averaged wind speed climatologies from hourly data, averaged over domains of the (a) southern Beaufort Sea (b) Chukchi Sea and (c) Bering Sea.

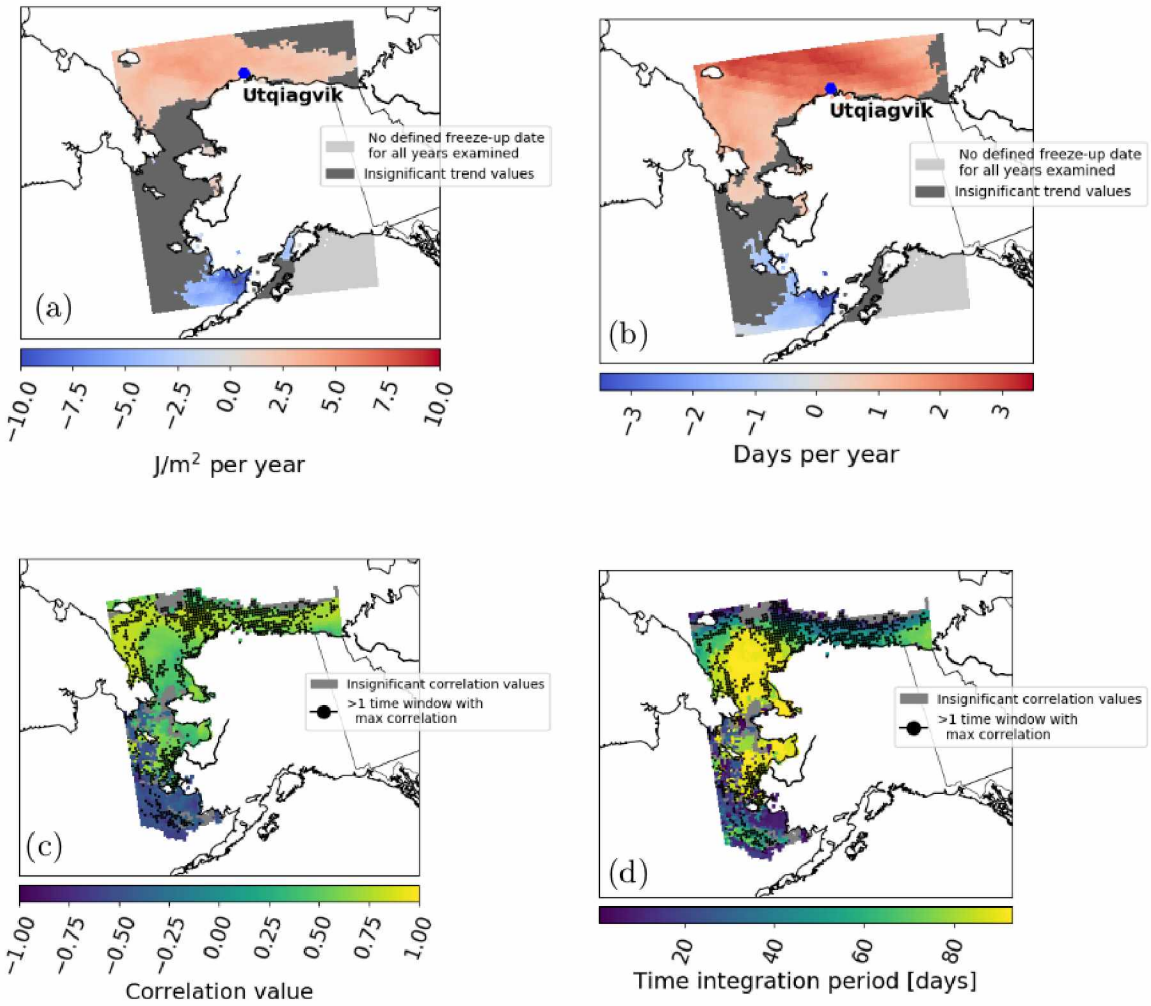

Figure 3.4: (a) Linear trend of the change in the annual cumulative wind energy input into the ocean over open water from 1979-2014. (b) Linear trend of annual open water duration from 1979-2014 defined as when sea ice concentration is less than 15%. (c) The maximum correlation value, compared across all time integration periods prior to freeze-up, for each grid cell. The dots represent time windows prior to freeze-up which had more than one equal correlation value. In this case, the correlation value from the longest time window was selected. (d) The time periods prior to freeze-up which showed the maximum magnitude correlation value with wind energy input and freeze-up timing. Dots represent those grid cells which had more than 1 time period with the maximum correlation value. In those cases, the longest time period is shown here.

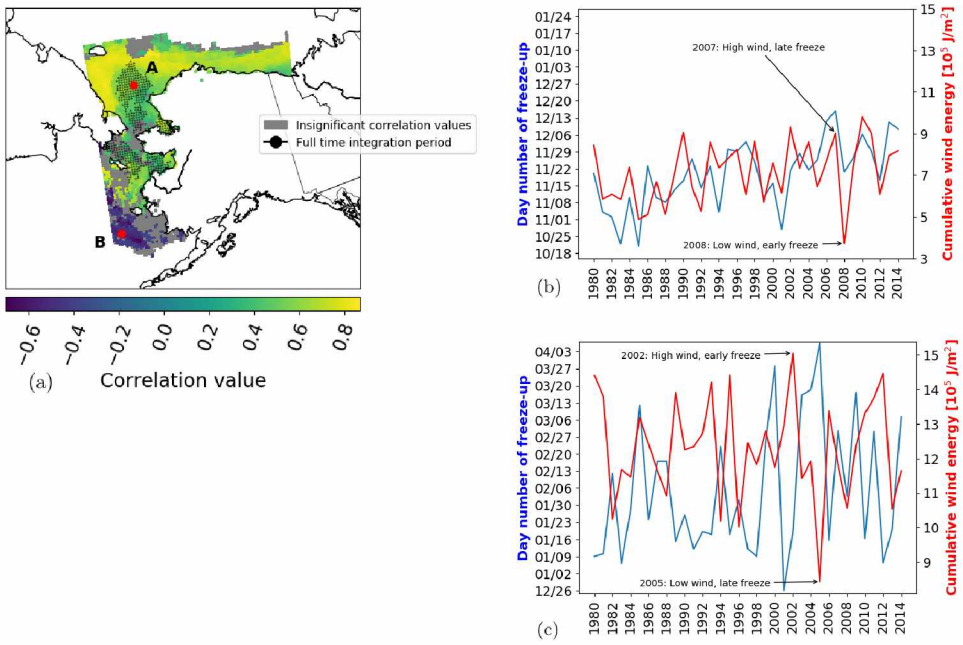

Figure 3.5: (a) The correlation values from the time integration period of 93 days prior to freeze-up and freeze-up timing of each grid cell. The points marked A and B are the locations of the case studies. The dots represent the grid cells where more than 80% of the years had a defined open water season length of at least 93 days. (b) The timeseries used to produce the correlation values at the Chukchi Sea location, Point A and (c) Bering location, Point B

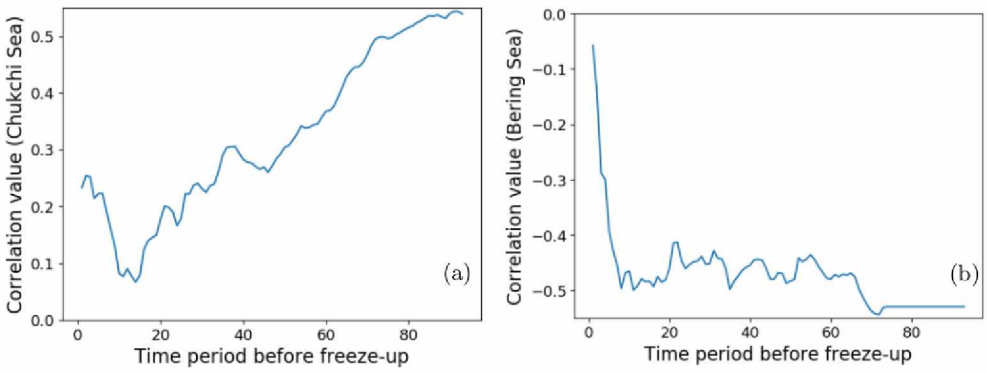

Figure 3.6: Correlation coefficient values between cumulative wind energy input and freeze-up timing for each time integration period examined from 1979-2014 for locations A (panel a) and B (panel b) (locations shown on the map in Figure 3.4). In (b) less than 80% of the years in the correlation calculation had an open water season length of at least 72 days, and so this correlation value is used for the subsequent time windows.

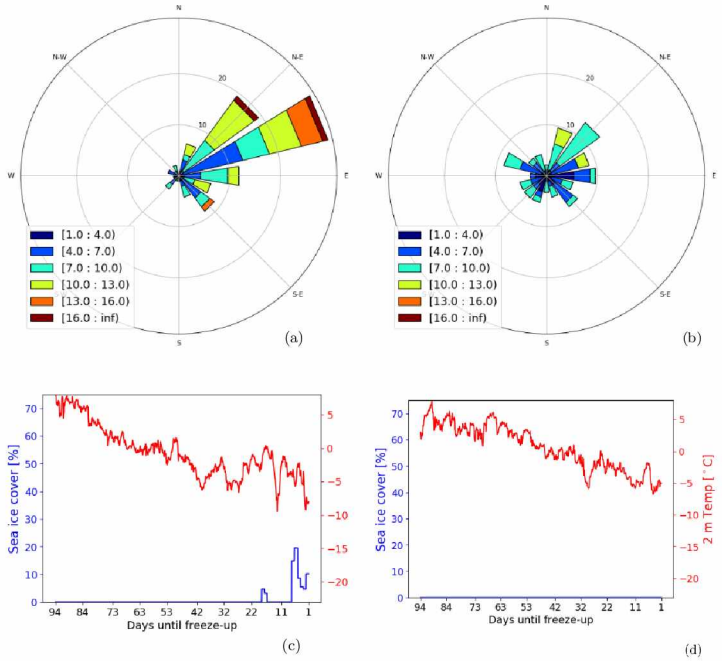

Figure 3.7: The daily averaged wind speeds and directions, and hourly 2 m surface air temperature with daily sea ice concentration in the 93 days before freeze-up (start of the longest ice-covered season) for the Chukchi Sea location (Point A in Figure 3.5) for the (a,c) high wind, late freeze-up year 2007, and (b,d) low wind, early freeze-up year 2008.

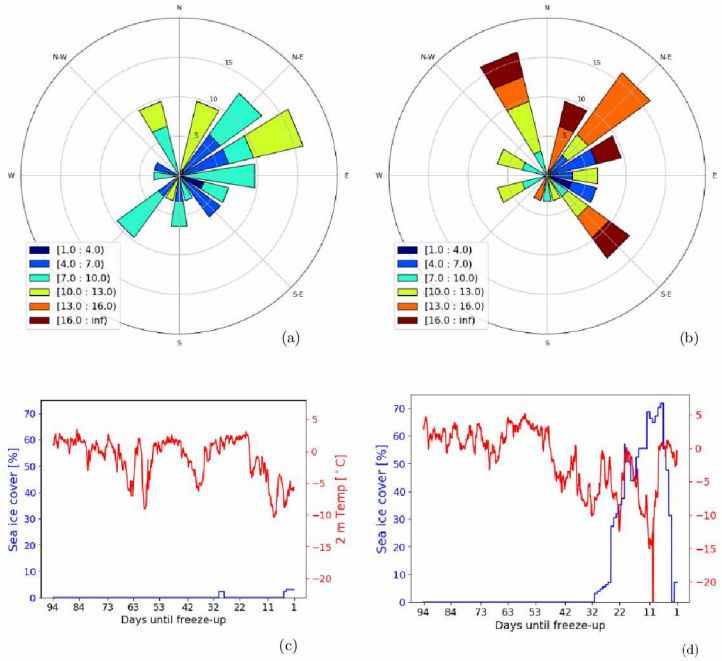

Figure 3.8: The daily averaged wind speeds and directions in the month prior to freeze-up (start of the longest ice-covered season) for the Bering Sea location (Point B in Figure 3.5) for the (a) low wind, late freeze-up year 2005, and (b) high wind, early freeze-up year 2002. Also given is the hourly 2 m surface air temperature with daily sea ice concentration in the 93 days before freeze-up for (c) 2005 and (d) 2002.

References

Aagaard, K., and A. Roach (1990), Arctic ocean-shelf exchange: Measurements in barrow canyon, *Journal of Geophysical Research: Oceans*, *95*(C10), 18,163–18,175.

Aksenov, Y., E. E. Popova, A. Yool, A. G. Nurser, T. D. Williams, L. Bertino, and J. Bergh (2017), On the future navigability of arctic sea routes: High-resolution projections of the arctic ocean and sea ice, *Marine Policy*, *75*, 300–317.

Bieniek, P. A., U. S. Bhatt, J. E. Walsh, T. S. Rupp, J. Zhang, J. R. Krieger, and R. Lader (2016), Dynamical downscaling of era-interim temperature and precipitation for alaska, *Journal of Applied Meteorology and Climatology*, *55*(3), 635–654.

Bourke, R. H., and R. G. Paquette (1976), Atlantic water on the chukchi shelf, *Geophysical Research Letters*, *3*(10), 629–632.

Dee, D. P., S. Uppala, A. Simmons, P. Berrisford, P. Poli, S. Kobayashi, U. Andrae, M. Balmaseda, G. Balsamo, P. Bauer, et al. (2011), The era-interim reanalysis: Configuration and performance of the data assimilation system, *Quarterly Journal of the royal meteorological society*, *137*(656), 553–597.

Denman, K., and M. Miyake (1973), Behavior of the mean wind, the drag coefficient, and the wave field in the open ocean, *Journal of Geophysical Research*, *78*(12), 1917–1931.

Hauri, C., P. Winsor, L. W. Juranek, A. M. McDonnell, T. Takahashi, and J. T. Mathis (2013), Wind-driven mixing causes a reduction in the strength of the continental shelf carbon pump in the chukchi sea, *Geophysical Research Letters*, *40*(22), 5932–5936.

Long, Z., and W. Perrie (2012), Air-sea interactions during an arctic storm, *Journal of Geophysical Research: Atmospheres*, *117*(D15).

Overeem, I., R. S. Anderson, C. W. Wobus, G. D. Clow, F. E. Urban, and N. Matell (2011), Sea ice loss enhances wave action at the arctic coast, *Geophysical Research Letters*, *38*(17).

Overland, J. E., and C. H. Pease (1982), Cyclone climatology of the bering sea and its relation to sea ice extent, *Monthly Weather Review*, *110*(1), 5–13.

Pease, C. H. (1980), Eastern bering sea ice processes, *Monthly Weather Review*, *108*(12), 2015–2023.

Price, J. F., J. Morzel, and P. P. Niiler (2008), Warming of sst in the cool wake of a moving hurricane, *Journal of Geophysical Research: Oceans*, *113*(C7).

Serreze, M. C., A. D. Crawford, J. C. Stroeve, A. P. Barrett, and R. A. Woodgate (2016), Variability, trends, and predictability of seasonal sea ice retreat and advance in the chukchi sea, *Journal of Geophysical Research: Oceans*, *121*(10), 7308–7325.

Stammerjohn, S., R. Massom, D. Rind, and D. Martinson (2012), Regions of rapid sea ice change: An inter-hemispheric seasonal comparison, *Geophysical Research Letters*, *39*(6).

Taylor, P. K., and M. J. Yelland (2001), The dependence of sea surface roughness on the height and steepness of the waves, *Journal of physical oceanography*, *31*(2), 572–590.

Woodgate, R. A., K. Aagaard, J. H. Swift, K. K. Falkner, and W. M. Smethie (2005), Pacific ventilation of the arctic ocean's lower halocline by upwelling and diapycnal mixing over the continental margin, *Geophysical Research Letters*, *32*(18).

Yang, J., J. Comiso, D. Walsh, R. Krishfield, and S. Honjo (2004), Storm-driven mixing and potential impact on the arctic ocean, *Journal of Geophysical Research: Oceans*, *109*(C4).

Zhang, X., and J. Zhang (2001), Heat and freshwater budgets and pathways in the arctic mediterranean in a coupled ocean/sea-ice model, *Journal of oceanography*, *57*(2), 207–234.

Chapter 4

Wind-driven changes in the heat content of the oceanic mixed layer using a 1-D column model

Rolph, R. J., Mahoney A. R., Walsh J. (2018, *in prep.*). Wind-driven changes in the heat content of the oceanic mixed layer using a 1-D column model. *Journal of Physical Oceanography.*

4.1 Abstract

Using a 1-D mixed layer model, we test the sensitivity of freeze-up timing of the surface ocean with different properties (temperature, salinity profiles) and changes in meteorological forcing. Temperature and salinity profiles (stratifications) come from an ice detection buoy deployed in 2015 in the north-east part of the Chukchi Sea and are assumed to be representative of stratifications during the freeze-up season for that region. Our results show that applying the same meteorological forcing on a shallower, warmer mixed layer with a gradual temperature gradient allows for enhanced warm water entrainment, followed by a subsequent increase in sensible heat loss. Higher average wind speeds in the three months prior to freeze-up result in an increased net heat loss due to vertical 1-D mixing by winds. Given that our 1-D simulations were not able to capture the freeze-up timing when compared to a reanalysis dataset, we conclude horizontal advective processes can dominate wind-driven vertical mixing to control the timing of freeze-up.

4.2 Introduction

A widening Arctic seasonal ice zone with increased open water periods allows for increased exposure to the winds. This region is beginning to get more attention as a region for enhanced vertical mixing (Rainville *et al.*, 2011). Under a declining sea ice cover, the surface ocean in the Arctic is experiencing changes in its level of wind-driven mixing. With its sea ice cover, the Arctic has previously been thought of as a highly stratified region where the surface waters are not subject to intense upper ocean mixing. Most of the mixing occurs during the shoulder seasons when stratification is relatively weak (Yang *et al.*, 2004). Since the formation of sea ice is happening later in the year, some associated air-sea fluxes should also be expected to change. For example, incident shortwave radiation will be even less at the time of freeze-up, as freeze-up is shifted toward the darker season of the year. Latent heat fluxes are increasing in concert with increasing sea surface temperatures (Yu and Weller, 2007). Sensible heat fluxes caused by turbulent mixing within the atmospheric boundary layer, an important mechanism for the ocean to lose heat during the fall freeze-up season (Inoue and Hori, 2011), is enhanced during periods of high surface wind speeds, and is also influenced by cloud cover (Ganeshan and Wu, 2016). Cloud cover can help trap heat at the surface, and thereby influence the ocean-atmosphere temperature gradient. In this study, we use a downscaled hourly reanalysis dataset from 1979-2014 to evaluate trends of the net surface heat flux and discuss what these trends mean in terms of sea ice formation. We further evaluate mechanisms of how surface heat fluxes play a role in sea ice growth.

Freeze-up timing across the Arctic has been linked with the timing of ice retreat in the previous season and varies by region (Stroeve *et al.*, 2016). Two-thirds of the variance for sea ice advance was found to be explained by changes in the July-September Bering Strait throughflow (Serreze *et al.*, 2016). Driving forces of sea ice advance, such as long-term changes in oceanic heat uptake due to the ice-albedo feedback, are discussed at larger spatial scales in studies such as Perovich *et al.* (2007). However, here we aim to narrow the scope to local vertical mixing mechanisms and how the water column changes its heat content and associated sensitivity to freeze-up timing.

The impact of storm-driven mixing on the upper Arctic Ocean has been examined previously (e.g. Toole *et al.* (2010) and Long and Perrie (2012)), but those studies examine conditions where sea ice was already present. What is lacking is how the timing of storms before freeze-up can influence the timing of freeze-up. Long and Perrie (2012) found a cooling of sea surface temperature in the coastal southern Beaufort sea by as much as 2°C, due to cooler water from a deeper level being mixed up towards the surface by a storm. However this may have been anomalous because whether or not the sea surface is cooled or warmed by mechanical mixing is dependent on the temperature of the entrained water compared to the existing water already in the mixed layer, which can fluctuate. For example, it has also been shown that a storm can cause a warming of the sea surface by penetrating through the halocline into the warm subsurface water below and mixing it upward (Yang *et al.*, 2004).

4.3 Data and Methods

4.3.1 Mixed layer model

The Price Weller Pinkel (PWP) model (Price *et al.*, 1986) is a 1-D mixed layer model that is initialized using a prescribed stratification (temperature and salinity profile) and forced with the meteorological components of wind stress, sensible heat flux, latent heat flux, net short wave, and net long wave radiation. It is essentially a model that has two types of forcings: buoyancy and wind or momentum flux. The heat, salt, and momentum conservation equations are each applied in 1-D formulations to the first vertical level (level spacings are set at 1 m in our experiments) and integrated forward in time by one timestep, where the flux profiles are then determined. The level of mixing, determined by the equations below, helps to determine these flux profiles. Starting with the initial stratification, the PWP model first removes static instability such that the ocean layers are uniformly mixed until the subsequent (deeper) layer contains a density greater than the layers above it (Equation 4.1).

$$\frac{\partial \rho}{\partial z} \geq 0 \tag{4.1}$$

The PWP model then uses a threshold bulk Richardson number to determine if the wind shear applied on the surface of the mixed layer should cause a deepening of the mixed layer. If the Bulk Richardson number (R_b) is less than 0.65 (Equation 4.2), the layer below the mixed layer depth is entrained and the resulting temperature and salinity properties are averaged evenly throughout the mixed layer. This process is repeated until the R_b equals or exceeds 0.65. When $R_b \geq 0.65$, the consumption of the turbulence is greater than the shear production, so the mixed layer is stable.

$$R_b = \frac{g\Delta\rho h}{\rho_0(\Delta V)^2} \geq 0.65 \tag{4.2}$$

To smooth the interface of the mixed layer properties and the properties below the mixed layer, a gradient Richardson number (Rg) threshold is also applied between the stratified region beneath the mixed layer to achieve shear flow stability. If Rg is below 0.25 (Equation 4.3), then the layers

at the base are partially mixed until Rg meets or exceeds 0.25.

$$R_g = \frac{g\partial\rho\ \partial z}{\rho_0(\partial V/\partial z)^2} \geq 0.25 \tag{4.3}$$

We initialize the model using stratification profiles taken from an ice-detection buoy deployed in 2015 ((Alaska Ocean Observing System, 2018), Section 4.3.3) and force with surface heat flux components from WRF-downscaled ERA Interim dataset (Section 4.3.2).

4.3.2 Wind stress and heat flux forcing: WRF-downscaled ERA Interim dataset

The European Centre for Medium-Range Weather Forecasts (ECMWF) interim reanalysis (ERA-Interim) dataset (Dee *et al.*, 2011) has been dynamically downscaled using an Advanced Research version of the Weather Research and Forecasting (WRF) regional model (Bieniek *et al.*, 2016). The period covered is 1979-2014 and has an hourly (daily for sea ice) resolution, with a spatial resolution of 20 km. The parent ERA-Interim dataset has a spatial resolution of 0.75 degrees (roughly 83 km), and a 6 hourly temporal resolution. The atmospheric model assimilates sea surface temperature and sea ice concentration products, and prescribes sea ice as a boundary condition. The reason the downscaled dataset was developed is to improve representation of temperature and precipitation around Alaska's complex coastline and varying terrain. Also, it is used to inform different stakeholders with high resolution weather and climate information.

4.3.3 Initial stratifications from freeze-up buoy

An ice-detection buoy was deployed on September 6, 2015, about 76 miles northwest of Wainwright in the Chukchi Sea, at 71.61°N and 161.4°W (Figure 4.1). It provided real-time data of temperature and salinity during the freeze-up season at depths of 0 m (surface), 1 m, 8 m, 20 m, 30 m, and 40 m. The data are freely available for download online (Alaska Ocean Observing System, 2018). We have selected stratifications from 2015 on September 22 and October 26 to initialize our mixed layer model, and these stratifications are labeled as 'Statified' and 'Unstratified' in our experiments, respectively. We have also initialized the model with a fresh surface layer of about 30 psu to test mixing under a high wind scenario from a very strong stratification, which can be caused by meltwater. We did not have a freeze-up detection buoy deployed overlapping with the timespan of the meteorological forcing we used to force the mixed layer model. So, we have assumed the profiles obtained by the freeze-up buoy to be representative of the profiles during the freeze-up season in the same location as the buoy. Further, the stratifications agree with profiles obtained from other sources, such as ship-based CTD casts in the same area. The initial profile labelled 'Stratified' also agrees with the T,S profiles obtained from CTD casts 2 months prior to the freeze-up buoy's recorded 'freeze-up date' (Chukchi Sea Environmental Studies Program, 2018).

4.3.4 Experimental set-up

Experiments were conducted using different meteorological forcing (different sensible and latent heat fluxes, wind stress, net short and longwave radiation flux) on the same initial stratification, and the differences in heat content of the resulting mixed layers were examined. The meteorological forcing was taken from the WRF-downscaled ERA-Interim dataset at the freeze-up buoy location (labelled in Figure 4.1 and described in section 4.3.3) for all open water timesteps. Since the date of freeze-up has changed dramatically in the last decade, recent years (since 2002) were selected to better represent the higher net surface fluxes being observed. The surface heat fluxes and wind stress components were extracted from these recent years with wind speeds which were the lowest (2008), highest (2010), and closest to the timeseries mean (2012). 93 days was chosen because shorter time integration periods showed lower correlation values between freeze-up timing and wind energy input, and higher correlation values occurred around 2-3 months (Chapter 3, Figure 3.6a). From the beginning timestep, surface heat fluxes and wind stresses were extracted for each hour of open water, until 15% ice cover was reached at the same location in the WRF-downscaled dataset. This resulted in a 93 day (hourly resolution) timeseries of surface heat fluxes and wind stresses for each year.

The model was then run using this meteorological forcing for each respective year on a single initial stratification (first stratified and then unstratified, see Section 4.3.3 for profile selection). So, there are three different years from which the meteorological timeseries were selected for forcing, and two different initial stratifications (making 6 model runs), plus an additional stratification with surface salinities near 30 psu. The experiments are referred to in the text as UL, UA, UH (Unstratified initial profile with Low, Average, High winds respectively), SL, SA, SH (Stratified initial profile with Low, Average, and High winds respectively), and 'fresh' initial profile. The 'fresh' experiment was run under the high wind scenario, initialized with one of the freshest stratifications collected by the freeze-up buoy. The high wind scenario was chosen for the fresh surface layer experiment to test if high winds are still able to break the high stratification and deepen the mixed layer. The resulting changes between the rate of upper ocean heat loss on the same initial stratification under the different wind scenarios are compared. To test sensitivity of freeze-up timing when using a different initial stratification, freeze-up timing between experiments using the same wind scenarios but different initial stratifications were also compared.

The mixed layer model is a simplified 1-D representation of the same water column in the WRF-downscaled dataset at the freeze-up buoy location. The 1-D model does not include any representation of horizontal advection. So, the difference between the length of the open water period in the WRF reanalysis dataset and how long the 1D mixed layer simulation takes to lose sensible heat content in the mixed layer can indicate the relative importance of advection. Further, the freeze-up timing of the WRF-downscaled dataset is defined as 15% ice cover, which happens after the mixed layer temperature has already reached freezing point.

We do not consider the differences in freeze-up timing at the buoy location between the WRF-downscaled ERA-Interim dataset and the mixed layer model simulation to impact our findings,

because our main purpose of using the mixed layer model is to evaluate how the differences in the net surface heat flux and wind speeds impact freeze-up timing of the water column. If the freeze-up timing of the ERA-Interim dataset are correlated with the rate of heat content loss in the mixed layer simulations, we can expect wind-driven vertical mixing to be a dominant mechanism for controlling freeze-up timing in reality. It is also worth noting that since the surface heat flux components are generated by the 3D model, they do somewhat capture advective processes as well, even though those processes are lost above and below the mixed layer in our 1-D model.

4.3.5 Calculation of cumulative wind energy

The wind energy input over open water was calculated for the open water timesteps of the meteorological variables taken from the WRF-downscaled ERA-interim data (see Section 4.3.4). The wind energy for those timesteps was calculated using the equation of Denman and Miyake (1973) (Equation 4.4), and multplied by 1 hour to approximate the integration of wind energy over each timestep.

$$\frac{\delta E}{\delta t} = \rho m C_d u^3 \tag{4.4}$$

where $\rho = 1.2 \frac{kg}{m^2}$ is air density, m = 10^{-3} is an efficiency factor, and $C_d = 10^{-3}$ is a drag coefficient, u is wind speed at 10 m above sea level. A similar technique was also performed in (Hauri *et al.*, 2013). The cumulative wind energy input was found by summing the wind energy input over the open water timesteps for each grid cell.

4.4 Results

4.4.1 Wind stress in relation to net heat fluxes

There has been an increase in average wind speed in the months prior to freeze-up by about 0.4 m/s per decade, as freeze-up moves into the fall storm season (Figure 4.2a). For all years where the wind speed prior to freeze-up is greater than the full timeseries (1980-2014) average, the average net heat flux is negative (ocean cooling). Prior to 2002, over the three months prior to freeze-up, most of the years have an average upper ocean warming, while in more recent years there has been an average upper ocean cooling. We found a significant increasing trend in the magnitude of the correlation between the wind speed and sensible heat fluxes, as well as the wind speed and latent heat fluxes in the months prior to freeze-up (Figure 4.2b). That is to say, the correlation between wind speed and the magnitude of the turbulent latent heat fluxes has grown stronger over the course of the study period. Net shortwave radiation also has a significant increasing trend in the magnitude of negative correlation with wind speeds in the 3 months prior to freeze-up.

The cumulative wind energy of the three meteorological timeseries chosen to force the mixed layer model start out similar in magnitude, with the relative differences most apparent near the end of each timeseries, closer to freeze-up. For the high wind season, the decrease in the cumulative net heat flux starts about 20 days before the sharp increase in the cumulative wind energy,

which starts around day 72 (red line in Figure 4.3).

4.4.2 Subsurface temperature maximum

Both the stratified and unstratified initial profiles (given as the dashed blue lines for temperature in Figure 4.4c,d respectively) have a subsurface temperature maximum. This maximum occurs between 20-27m for the stratified initial profiles and between 35-40m for the unstratified initial profiles. One important difference of the subsurface temperature maximum between the stratified and unstratified profiles is that it occurs at the base of the mixed layer in the stratified profile, with cooler water underneath the maximum temperature. The temperature maximum at the base of the unstratified (deeper) mixed layer does not have any cooler water beneath. This difference has consequences for changes in mixed layer temperature when the subsurface water is entrained. By the end of each experiment, the mixed layer cooled except for UA. That experiment resulted in a slight warming of about 0.1°C (solid green line in Figure 4.4d). For the other experiments, as the mixed layer cools, the subsurface temperature maximum becomes more pronounced (solid lines in Figure 4.4c,d). The greatest deepening occurred with the experiments of the 'high wind season', which also exhibited the most surface cooling for both the stratified and unstratified initial conditions. For all of the stratified (and fresh) experiments, the temperature below the subsurface temperature maximum increased. The mixed layer of UL cooled to approximately the same temperature as UH (Figure 4.4d). This is in contrast to the stratified initial profile experiments where SL resulted in a mixed layer substantially warmer than SH, even more than the freshest initial stratification (Figure 4.4c). The fresh initial mixed layer under the high wind forcing still resulted in a deepening, even though the water column started out as relatively stable due to the substantial fresh surface layer (Figure 4.4a,c).

4.4.3 Heat content of the mixed layer and differences in wind energy input

The integrated cumulative wind energy for each of the three wind forcings relative to the excess (sensible) heat content of the respective mixed layers are given in Figure 4.5. The stratified experiments (solid black lines) show higher variability in the excess heat content of the mixed layers compared to the unstratified experiments (dashed black lines). The experiment with the fresh surface layer (blue line labelled 'fresh' in Figure 4.5c) had fluctuations in excess heat content between that of the very unstratified and stratified higher salinity experiments. The heat content increased at the fastest rate for the high wind season, with a sharp drop around day 38 and a peak around day 50. The high wind season also showed the fastest decrease in heat content of the mixed layer, which resulted in the lowest overall heat content compared to the seasons with lower average wind speed. However, the high wind season did not show any rapid change in the rate of mixed layer cooling when there was a sharp increase in wind energy input around day 72 (red line in Figure 4.5c).

Considering all years (not just the ones chosen as forcing for the model in this study) from 1980-2014, the cumulative wind energy in the months prior to freeze-up is positively correlated

with delayed freeze-up timing (Figure 4.6). The freeze-up timing in this case is defined as 15% sea ice cover at the buoy location in the ERA-Interim dataset.

4.5 Discussion

4.5.1 Shift in net heat flux and wind speeds in the months prior to freeze-up

There has been a general shift from an average net positive heat flux (ocean gaining heat) over open water in the 3 months prior to freeze-up, to an average net negative heat flux (blue line in Figure 4.2a). In other words, although freeze-up is happening later, it also appears to be happening faster. One reason is that the downward shortwave flux is decreasing as freeze-up is delayed toward the darker part of the year. Another reason is due to the increased sensible heat flux from the ocean to the atmosphere as there are more days without sea ice cover, and so heat is more readily lost from the ocean.

The faster rate of cooling of the mixed layer coincides with the increase in wind speeds (black line in Figure 4.2). Although decreased incoming shortwave radiation is a factor in ocean cooling, increased wind speeds will increase the rate of turbulent heat released from the ocean. In addition, we have found significantly increasing magnitudes of correlation between wind speed and turbulent heat fluxes in the months prior to freeze-up (Figure 4.2a). We interpret this to be a consequence of the ice concentration during the 3-month period prior to freeze-up becoming more consistent (i.e. consistently zero), thereby allowing wind speed to have a stronger effect on the magnitude of the turbulent heat fluxes. High winds are often associated with storms which bring in cloud cover, and therefore can increase the longwave radiation. However, we find increased longwave radiation is not showing any significant change in its contribution to the net heat flux (black line in Figure 4.2b).

Sources of error in the ERA-Interim radiation products will contribute to uncertainty in the amount of excess heat content in the mixed layer. The error associated with the turbulent heat fluxes is amplified with increased wind speeds, and so also is larger in recent years. In addition, net heat fluxes are slightly overestimated in ERA-Interim (Dee *et al.*, 2011), which leads to an overestimation of oceanic heat uptake in that dataset (but improved since ERA-40) (Balmaseda and Mogensen, 2010). The excess ocean heat uptake was found to be highest in convective tropical regions but was not evaluated specifically in the Arctic. ERA-Interim has indicated diminishing surface wind speeds by 0.1 m/s over the 10 year period from 1992-2002, and after 2002, the trend is reversed. After 2002, the ECMWF operational forecast system also shows increasing surface wind speeds over the oceans, which is related to the evolution of the observing system (Dee *et al.*, 2011). The changes in the wind speeds prior to freeze-up is 0.4 m/s per decade, four times larger than the proposed changes in the surface wind speeds due to changes in the observing system for ERA-Interim. It is important to note here that the ERA-Interim dataset is the parent dataset which provides forcing for the WRF-downscaled regional atmospheric model over Alaska, and the trend reported by Dee *et al.* (2011) does not necessarily reflect those changes found in WRF-downscaled output.

4.5.2 Increased variability in heat content with a shallower mixed layer

Sharp changes in excess heat content of the mixed layer (black lines in Figure 4.5) are caused by changes in mixed layer depth. When water is entrained from below, it adds to the total heat content of the mixed layer which must be lost before freeze-up can occur. Therefore, under similar net heat fluxes, a rapid deepening of the mixed layer will cause it to take longer to reach freezing temperature than a mixed layer which has remained shallow. Since wind-driven mixing tends to deepen the mixed layer, it is reasonable to expect windier seasons to have a higher excess heat content than the less windy seasons in the months prior to freeze-up, as is the case for all of the stratified experiments until about day 50 (Figure 4.5). The experiment with the fresh initial mixed layer (blue line in Figure 4.5c) has comparable excess heat content with SA at approximately day 50. Even though SA had lower cumulative wind energy as forcing, the fresher surface layer inhibited some of the wind mixing by providing a stronger stratification. During the sharp increase of cumulative wind energy of the high wind season around day 71, there was not a coincident sharp decrease in the net heat flux (Figure 4.3). If this sharp increase in the cumulative wind speeds were to happen earlier on in the season, for example, around day 1-50, this would not be the case. Earlier in the season prior to freeze-up, the mixed layer would be shallow enough for the increase in wind speeds to cause a deepening and therefore an increase in the excess heat content of the mixed layer. However, if the surface layer is fresh enough, it will be more difficult for the winds to deepen the mixed layer due to the increased stratification. Very fresh surface layers can be caused by ice melt or runoff from rivers. Heavy rains may impact the salinity of the surface during the freeze-up season.

4.5.3 Advective processes and freeze-up timing

Since the mixed layer model chosen in this study is 1-D column model, it does not capture the processes of horizontal heat advection in the water column. The same meteorological conditions caused a freeze-up (defined as 15% sea ice cover) at the buoy location in the WRF-downscaled ERA interim dataset, but the 1-D column model still had excess heat content in the mixed layer (Figures 4.4 and 4.5). This shows that advective processes are important to carry heat away from the water column in order for it to reach freezing temperature. Since the meteorological conditions used were from a 3-D reanalysis dataset, advective processes in the atmosphere were taken into account. This leaves the ocean advective processes as an important factor in removing heat from the water column.

For all years from 1980-2014, there is a significant positive correlation at the buoy location between cumulative wind energy over open water in the months prior to freeze-up and when 15% sea ice cover is obtained in the ERA-Interim dataset (Figure 4.6). Besides the advective mechanisms discussed above, changes in the meteorological forcing (e.g. selecting different years than the 2008, 2010, and 2012 chosen in this study) will produce different mixed layer results. In a 1-D vertical system, our results show increased cumulative wind energy caused the high wind season

(red dot marked on Figure 4.6) to result in the fastest (Figure 4.5) and most cooling (Figure 4.4) of the mixed layer. However, according to the ERA-interim dataset, the high wind season transitioned from open water to ice cover around the same time as the low wind (compare red dots in Figure 4.6) and the average wind (green dot in Figure 4.6) freeze-up seasons. Given the general trend (from 1980-2014) that increased cumulative wind energy results in a delayed freeze-up (Figure 4.6), we may expect the selected years to have high oceanic advective processes not captured in our 1-D model which dominate their freeze-up timing.

4.6 Conclusions

We have run a 1-D vertical mixing model to examine the impacts of wind-driven mixing on the heat content of the mixed layer. We have found that, when horizontal advective processes are excluded, stronger winds promote heat loss out of the ocean. We have also found, in the 3 months prior to freeze-up, that latent and sensible heat fluxes are becoming more correlated with wind speed in recent years. This is due to the turbulent heat fluxes being less controlled by changes in surface cover (e.g. open water and ice cover) as the surface cover becomes more consistently open water and more controlled by changes in wind speed. This may not necessarily be the case for more southerly latitudes than the location examined here, such as places where the open water season length from 1979-2014 has been consistently at least three months long.

We have found a significant positive correlation between freeze-up timing and cumulative wind energy input for the overall time period of 1980-2014 in the north east part of the Chukchi Sea. Given this positive correlation and under the same initial stratification, we would have expected the more windy season to lose heat from the mixed layer later than the less windy seasons. Since this was not the case in this 1-D mixing study, we can conclude that advective processes not captured by the 1-D model are important in driving heat loss out of the mixed layer. We have also found that variability in the sensible heat content of the mixed layer is lower when the stratification is very weak, since wind-driven deepening is less likely to occur.

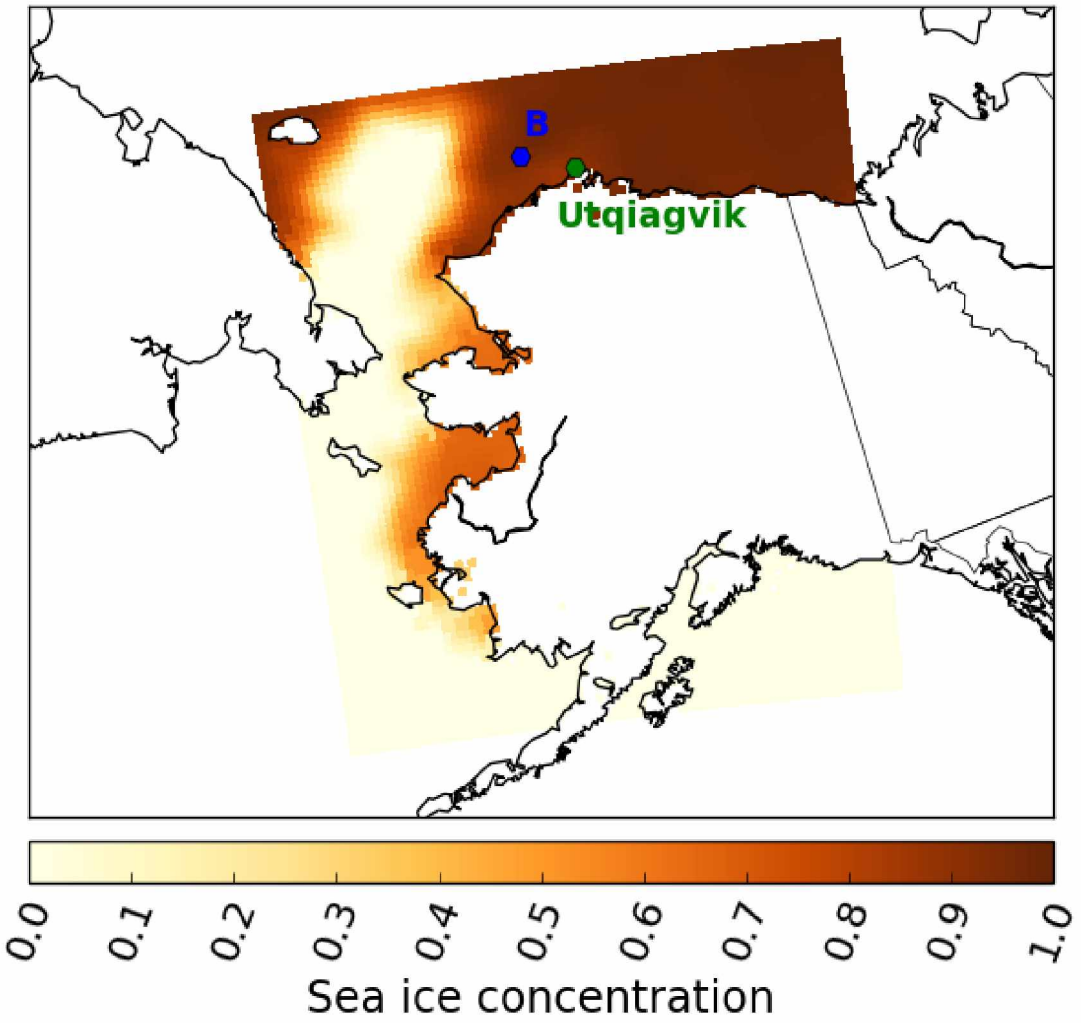

Figure 4.1: Location of meteorological forcing for experiments and stratification information from the freeze-up buoy (marked by B). Sea ice concentration from ERA-Interim in early November 2011.

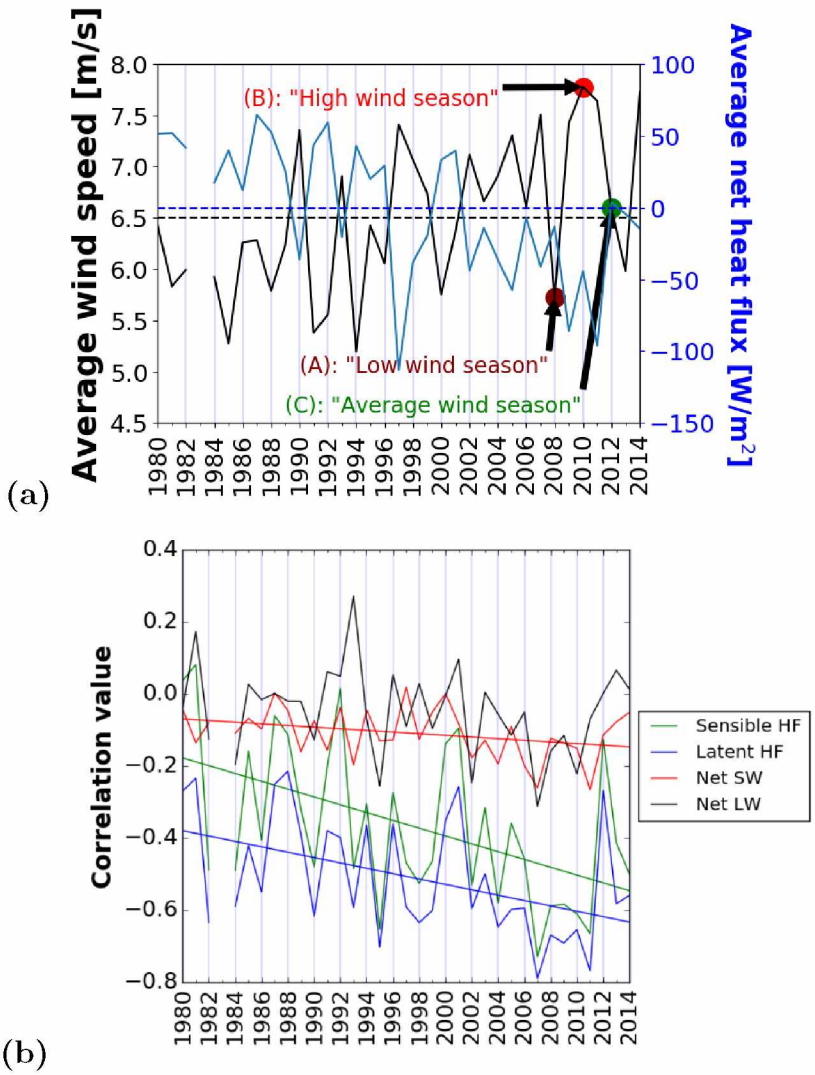

Figure 4.2: (a) Average wind speeds at the freeze-up buoy location in the time period 93 days prior to freeze-up. Wind speeds over sea ice cover are included if the open water period for the respective year was less than 3 months long. 1983 shows no value because there was no recorded freeze-up date (year-round ice cover) at the buoy location for that year. (b) Correlations between the components of heat fluxes and average wind speeds in the three months prior to freeze-up. Significant negative trends in the correlation values were found for the net shortwave, latent , and sensible heat fluxes. Wind speeds averaged from hourly WRF-downscaled ERA-Interim data.

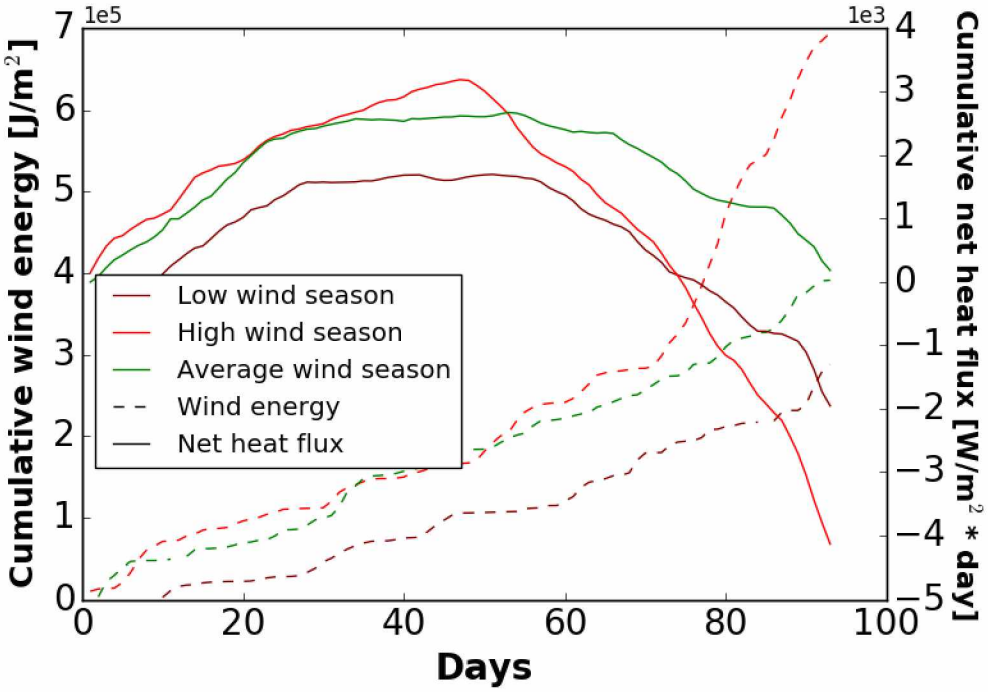

Figure 4.3: Cumulative net heat fluxes over open water and cumulative wind energy input over open water of the meteorological forcing for the PWP mixed layer model. Negative net heat flux refers to mixed layer cooling.

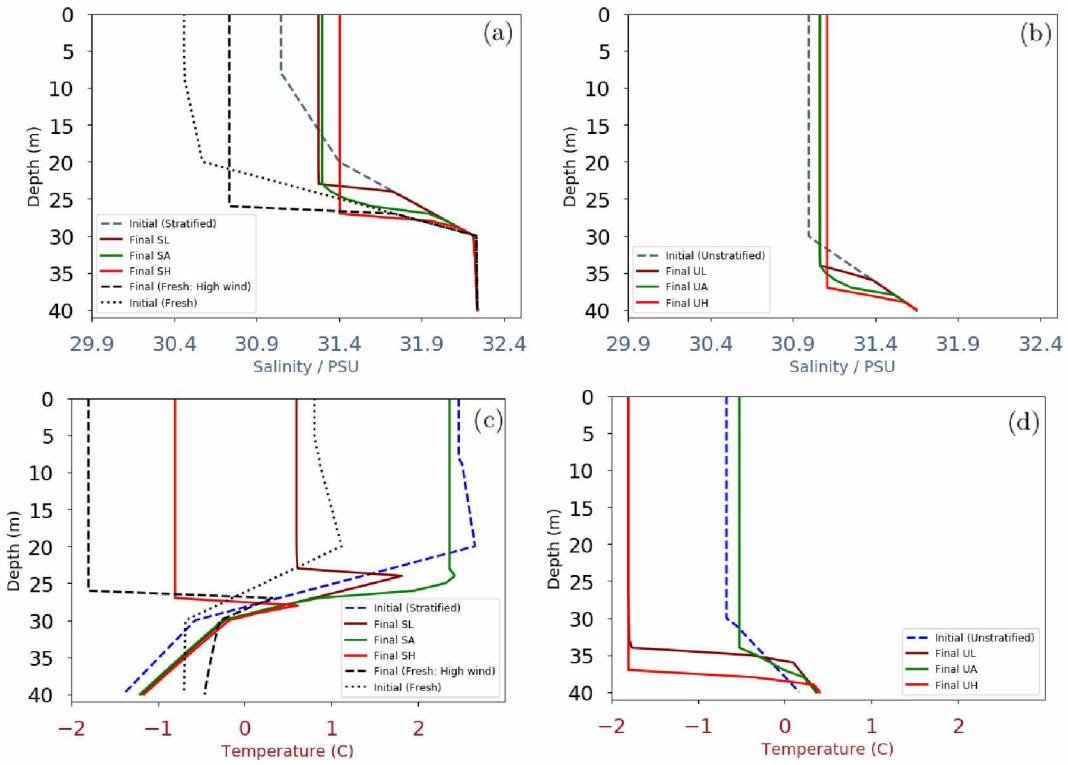

Figure 4.4: Salinity (a,b) and temperature (c,d) profiles of the mixed layer model experiments for the initially stratified (left panels) and initially unstratified (right panels) experiments. Heat fluxes and wind stresses in the time period before freeze-up are from WRF-downscaled ERA-Interim data at the location of buoy site (shown in Figure 4.1). The seafloor is approximately 40 m at the buoy location.

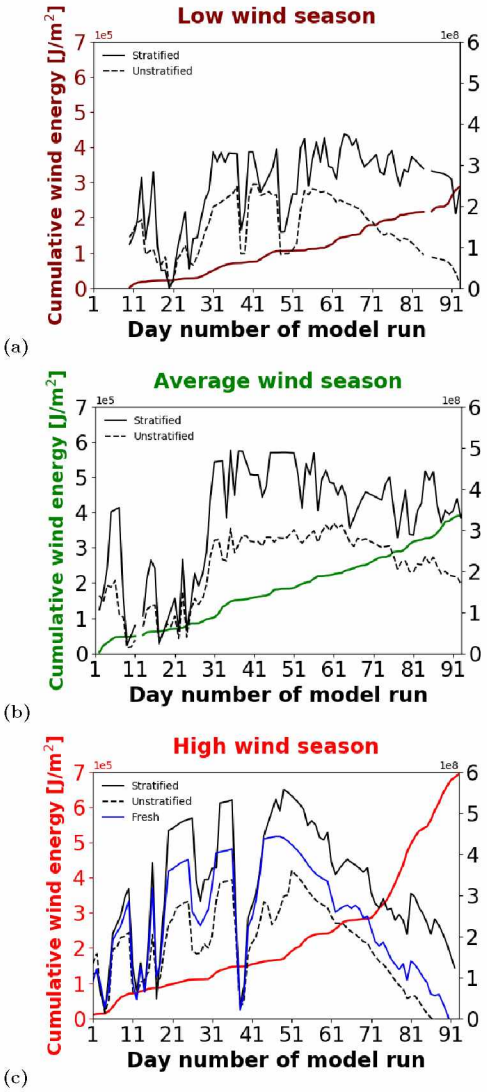

Figure 4.5: Cumulative wind energy and excess heat content of the mixed layer for the six experiments of the low (a), average (b), and high (c) wind seasons. Dashed lines are experiments initialized with the unstratified initial temperature and salinity profile, solid lines are those experiments initialized with the stratified profiles.

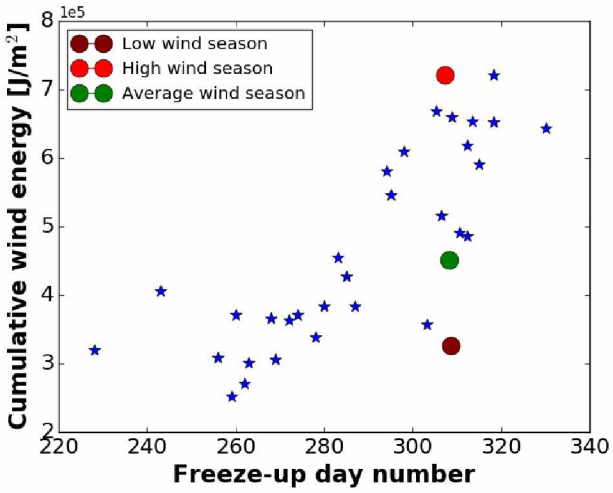

Figure 4.6: Hourly cumulative wind energy over open water and freeze-up day number for freeze-up buoy location (shown in Figure 4.1. Freeze-up day number is defined as when the location of the freeze-up buoy reached 15% sea ice concentration in the ERA-Interim dataset. There is a general positive correlation between delayed freeze-up timing and increased wind energy input into the water column. Low, average, and high wind seasons in the months prior to freeze-up are given by the dark red, green, and bright red dots respectively.

References

Alaska Ocean Observing System (2018). Ice Detection Buoy. http://www.aoos.org/ice-detection-buoy/. Accessed: 2017-07-30.

Balmaseda, M. and Mogensen, K. (2010). *Evaluation of ERA-Interim forcing fluxes from an ocean perspective*. European Centre for Medium Range Weather Forecasts.

Bieniek, P. A., Bhatt, U. S., Walsh, J. E., Rupp, T. S., Zhang, J., Krieger, J. R., and Lader, R. (2016). Dynamical downscaling of era-interim temperature and precipitation for alaska. *Journal of Applied Meteorology and Climatology*, **55**(3), 635–654.

Chukchi Sea Environmental Studies Program (2018). CSESP. http://www.chukchiscience.com/Downloads/. Accessed: 2018-04-19.

Dee, D. P., Uppala, S., Simmons, A., Berrisford, P., Poli, P., Kobayashi, S., Andrae, U., Balmaseda, M., Balsamo, G., Bauer, P., *et al.* (2011). The era-interim reanalysis: Configuration and performance of the data assimilation system. *Quarterly Journal of the royal meteorological society*, **137**(656), 553–597.

Denman, K. and Miyake, M. (1973). Behavior of the mean wind, the drag coefficient, and the wave field in the open ocean. *Journal of Geophysical Research*, **78**(12), 1917–1931.

Ganeshan, M. and Wu, D. L. (2016). The open-ocean sensible heat flux and its significance for arctic boundary layer mixing during early fall. *Atmospheric Chemistry and Physics*, **16**(20), 13173–13184.

Hauri, C., Winsor, P., Juranek, L. W., McDonnell, A. M., Takahashi, T., and Mathis, J. T. (2013). Wind-driven mixing causes a reduction in the strength of the continental shelf carbon pump in the chukchi sea. *Geophysical Research Letters*, **40**(22), 5932–5936.

Inoue, J. and Hori, M. E. (2011). Arctic cyclogenesis at the marginal ice zone: A contributory mechanism for the temperature amplification? *Geophysical Research Letters*, **38**(12).

Long, Z. and Perrie, W. (2012). Air-sea interactions during an arctic storm. *Journal of Geophysical Research: Atmospheres*, **117**(D15).

Perovich, D., Light, B., Eicken, H., Jones, K., Runciman, K., and Nghiem, S. (2007). Increasing solar heating of the arctic ocean and adjacent seas, 1979–2005: Attribution and role in the ice-albedo feedback. *Geophys. Res. Lett*, **34**, L19505.

Price, J. F., Weller, R. A., and Pinkel, R. (1986). Diurnal cycling: Observations and models of the upper ocean response to diurnal heating, cooling, and wind mixing. *Journal of Geophysical Research: Oceans*, **91**(C7), 8411–8427.

Rainville, L., Lee, C. M., and Woodgate, R. A. (2011). Impact of wind-driven mixing in the arctic ocean. *Oceanography*, **24**(3), 136–145.

Serreze, M. C., Crawford, A. D., Stroeve, J. C., Barrett, A. P., and Woodgate, R. A. (2016). Variability, trends, and predictability of seasonal sea ice retreat and advance in the chukchi sea. *Journal of Geophysical Research: Oceans*, **121**(10), 7308–7325.

Stroeve, J. C., Crawford, A. D., and Stammerjohn, S. (2016). Using timing of ice retreat to predict timing of fall freeze-up in the arctic. *Geophysical Research Letters*, **43**(12), 6332–6340.

Toole, J. M., Timmermans, M.-L., Perovich, D. K., Krishfield, R. A., Proshutinsky, A., and Richter-Menge, J. A. (2010). Influences of the ocean surface mixed layer and thermohaline stratification on arctic sea ice in the central canada basin. *Journal of Geophysical Research: Oceans*, **115**(C10).

Yang, J., Comiso, J., Walsh, D., Krishfield, R., and Honjo, S. (2004). Storm-driven mixing and potential impact on the arctic ocean. *Journal of Geophysical Research: Oceans*, **109**(C4).

Yu, L. and Weller, R. A. (2007). Objectively analyzed air–sea heat fluxes for the global ice-free oceans (1981–2005). *Bulletin of the American Meteorological Society*, **88**(4), 527–539.

Chapter 5

Conclusion

5.1 Implications for a lengthened open water period

Here we briefly discuss the answer to Question 1 of the Introduction (Chapter 1): "How are coastal communities affected by changes in the length of the open water season and how can we assess these impacts using large scale datasets?". Using simple physical thresholds identified from local observations, we have shown that large-scale datasets (such as the WRF-downscaled ERA-Interim Reanalysis dataset) can be used to develop climate-related indices on a local scale. The development of indices in general makes information about a changing climate easier to quantify, and also allows for comparison across communities. We have found mostly faster rates of change in the northern coast of Alaska, in Utqiaġvik (previously Barrow), compared to the more southern communities of Kotzebue and Shishmaref. The increasing number of false freeze-ups and break-ups impact communities by causing disruption in the transition between boat and snow machine and the use of sea ice as a safe platform for hunting. The number of false freeze-ups in recent years has been increasing, particularly in Shishmaref. The increases in false freeze-ups and break-ups in recent years are likely to represent a 'new normal' if these trends continue.

The implications for an earlier break-up and later freeze-up varies by community. Kotzebue has already noticed a shorter subsistence hunting season of bearded seal in late spring, because the sea ice recedes earlier, so the animals begin to migrate north earlier than in the past, following the sea ice (Whiting, personal communication). Other locations have different consequences for accessibility of walrus in response to a sea ice cover that is receding earlier. For example, with negative sea ice concentration anomalies, the communities of Savoonga and Gambell on St. Lawrence Island have more favorable or near-average hunting conditions for walrus, respectively (Kapsch *et al.*, 2010). High sea ice concentration becomes a problem when ice is pushed and piled up onto or near the coast, making it difficult for hunters to launch their boats from the shore (Kapsch *et al.*, 2010). The presence of sea ice can also have benefits, such as damping erosion-causing wave action along the coastline (Barnhart *et al.*, 2014). Utqiaġvik has more infrastructure than the other two communities examined (Kotzebue and Shishmaref), which would lead to greater economic loss of enhanced coastal erosion driven by a longer open water season. Shishmaref, being a barrier island, must eventually find an entirely new location due to increased shoreline erosion.

In terms of impacts on transportation, the number of 'boatable' days is not increasing as much as one might expect from the rapid increases in total open water season length. This is due to higher winds typically found during the delayed fall freeze-up (Chapter 3, Figure 3.3), which can make boat launches and travel unsafe. Utqiaġvik shows the greatest change in the increase in the number of open water days, but also the greatest increase in the number of days deemed 'too windy' for boat travel by hunters (Chapter 2, Figure 2.7).

The number of wind events capable of significant shoreline erosion has also increased. The longer open water period has allowed for more time for fall storms to generate higher waves without the cap of sea ice cover. We have found the greatest increases in geomorphologically signifiant wind events in Utqiaġvik, but the greatest number of these wind events occurs in Shishmaref, followed by Kotzebue. This is mainly due to the longer open water season in the more

southern communities. However, the increase in the number of these wind events in Utqiaġvik is significant. The increases in the number of these high wind events in a direction promoting water setup along the coastline is greatest in Shishmaref, which will further worsen the already existing problem of erosion there.

In summary, it is important to evaluate not only the differences in the number of days of open water between these communities, but also the associated consequences, such as changes in the number of false freeze-ups/break-ups, freeze-up/break-up timing, and wind events over open water. These changes have been compiled into locally-relevant indices in this thesis, and it is discussed in Chapter 2 how they can be an important metric to elucidate the community-relevant trends of climate change. The methods used to develop these indices can be applied at any Arctic community. However, it should be noted that the consequences of the indices (e.g. freeze-up timing) can be very different depending on which community is being evaluated (Kapsch *et al.*, 2010). We have chosen only to examine the three Alaska coastal communities of Utqiaġvik, Kotzebue, and Shishmaref, but it would be valuable to examine differences between other communities as well, and to compare across communities in Arctic regions other than Alaska.

Consequences for communities are not the only aspects of a lengthened open water season evaluated in this thesis. The lengthened open water season allows for more wind to be applied to the upper ocean and so increases the amount of wind energy put into the upper ocean. This cause changes in the timing of freeze-up (Chapter 3) and heat content of the upper ocean (Chapter 4), which are discussed in the next sections.

5.2 Impacts of increasing wind speeds in the 3 months prior to freeze-up

To begin to answer Question 2 of the Introduction (Chapter 1): "What are the implications for increased wind stress over open water due to delayed freeze-up?" we evaluated trends in the wind speeds particularly in the months prior to freeze-up, and have found that the wind speeds have increased (Figure 3.2). In Chapter 3, we found that the wind climatologies for Alaska waters have not changed significantly during the fall storm season (Figure 3.3). The delay of freeze-up into the windier part of the year is causing the wind speeds prior to freeze-up to increase. We also showed that a more windy season 2-3 months prior to freeze-up is significantly and positively correlated with delayed freeze-up timing in the Chukchi Sea (Figure 3.5). In the Bering Sea, there is a negative correlation, which is an indicator that winds promote freeze-up. In the case studies examined, we found that sea ice advection is an important mechanism for determining the time of freeze-up in the Bering Sea. Strong northeasterly winds can upwell warm, salty, Atlantic water up onto the Chukchi shelf (Bourke and Paquette, 1976; Aagaard and Roach, 1990) and can be provided as a possible explanation for the positive correlation in the Chukchi Sea. Further, the case study evaluated squarely in the middle of the shelf shows high winds coming from the dominant northeasterly wind direction (Figure 3.7a), which suggests the upwelling of warm water as a possible contributing mechanism for the later freeze-up observed during that year.

Outgassing of CO_2 is another consequence of increased wind-driven mixing in the Chukchi

Sea region (Hauri *et al.*, 2013). Although the Chukchi is currently viewed as a carbon sink (Mathis and Questel, 2013), increasing wind speeds in the months prior to freeze-up may increase the overall carbon outgassing budget in the Chukchi Sea. Related to quantifying these surface carbon fluxes, the lengthened open water season in conjunction with increasing wind speeds highlights the need to accurately parameterize turbulent surface fluxes over the ocean.

5.3 Winds and mixed layer heat content

The more specific mechanisms of how storms and upper ocean mixing can subsequently influence the timing of freeze-up (see Questions 3 and 4 of the Introduction, Chapter 2) are discussed in Chapter 4. We have shows how differences in ocean stratification can change the rate of heat loss out of the upper ocean's mixed layer (Chapter 4). The stratification of the upper Arctic ocean changes with the seasons (e.g. density changes from freshening by meltwater, changes in temperature from availability of shortwave radiation). Two to three months prior to freeze-up tends to be less stratified than immediately prior to freeze-up (Chukchi Sea Environmental Studies Program, 2018). This is due to warmer and fresher surface waters a few months prior when compared to immediately before freeze-up. Since the upper ocean is more likely to deepen when it is slightly more stratified (typically 2-3 months prior to freeze-up) than an already deep mixed layer (typical immediately prior to freeze-up), it follows that a more windy season in the 2-3 months prior to freeze-up will result in a greater change of mixed layer depth. Since the entire mixed layer must reach freezing temperature before sea ice can develop, adding more water to the mixed layer will require more energy (heat) loss in order to reach freezing temperature. This is the mechanism, as we have shown using a mixed layer model and downscaled atmospheric forcing in Chapter 4, which leads to an increased heat content under a more windy season in the 2-3 months prior to freeze-up.

Although the increased heat content resulting from winds entraining more water volume into the mixed layer is an important mechanism, we also found that a 1-D mixing model was not able to reproduce a delayed freeze-up in response to high wind conditions (Chapter 4). We therefore conclude that processes not accounted for by the model, such as advection, are likely to be at least as important. The mixed layer still had more heat to be lost before freeze-up could occur in most of the simulations, but it had already reached 15% sea ice cover in the same location according to the ERA-Interim dataset. Therefore, it can be concluded the advective processes not captured in the PWP 1-D mixing model are very important in controlling freeze-up timing. Advection of sea ice has been shown to be important in the Bering Sea case studies of Chapter 3.

5.4 Applicability of freeze-up timing on a pan-Arctic scale

The start of this thesis (Chapter 2) explores the broader implications for changes in the open water season length, freeze-up and break-up timing on people within selected Arctic communities by methods which can be made applicable to other communities. The necessary data to make comparisons across Arctic communities located outside the Chukchi Sea are available, including

wind speed and direction data, as well as sea ice concentration. However, due to some limitiations of satellite-derived sea ice concentration products near the coastline, as well as limitations in the definition of freeze-up timing, it is also important to incorporate observations from community members (e.g. Johnson and Eicken (2016)). The impact of winds on the timing of freeze-up described in Chapters 3 and 4 are likely to be varied in different areas of the Arctic because the distribution of high wind events is not uniform across the Arctic region (Hughes and Cassano, 2015). For example, the Norwegian Sea and Barents Sea have more strong wind events than in the Kara Sea. We can expect the impacts of wind-driven upper ocean mixing to be a more significant influence on the timing of freeze-up in those more windy regions.

Coastal communities can have highly variable oceanic conditions, and also differences in their exposure to the open ocean, depending on geographic position. For example, Kotzebue Sound is highly influenced by river runoff from the Kobuk, Noatak, and Selawik Rivers. Utqiaġvik, on the other hand, is exposed to drifting pack ice, the Alaska Coastal Current and Beaufort Gyre. Other communities in the Arctic, such as those located in the Canadian Archipelago, are subject to thicker sea ice and more protected from larger-scale ocean currents. The variability in the oceanic conditions between these communities is one factor which causes differences in the implications for changes in freeze-up timing. For example, water setup along the coastline and the significant height of wind waves are enhanced by increasing fetch (Asplin *et al.*, 2012), so those communities which are geographically surrounded by more land and less mobile sea ice (e.g. Canadian Archipelago) are less likely to experience such dramatic erosion rates due to increases in water setup. These factors should be taken into account when developing timeseries of the same indices for other Arctic communites not examined here. Perhaps more useful indices to measure impacts of sea ice change on Arctic communities located in the Canadian Archipelago are changes in accessiblity and feasibility of Arctic tourism. Sea ice decline has made Arctic tourism more accessible, with the fastest growing types of ships being pleasure (non-commercial) boats (Johnston *et al.*, 2017). Increased tourism in the Arctic is a recent topic of interest, and the impacts of tourism on Arctic communities need more attention (Ford and Pearce, 2010).

5.5 Outlook: Indirect and direct community impacts of sea ice change

We have examined the physical processes associated with wind-driven mixing of the upper ocean (Chapter 4), which have been shown to be important to control the heat content of the upper ocean, but other processes (e.g. advection) have also been shown to influence the timing of freeze-up (Chapter 3). Changes in the timing of freeze-up has direct impacts on coastal communities in terms of accelerated erosion rates, when the ice is safe for travel, and when the sea ice is accessible to subsistence hunters (Chapter 2). However, direct impacts do not address all of the impacts sea ice change has on Arctic communities. Economic changes can be brought about by changes in the levels of activities such as increased tourism (Johnston *et al.*, 2017) or a potential need to find bigger boats to adapt to the increased number of open water days in windy conditions (Chapter 2). Such changes lead to indirect impacts of a lengthened open water season on Arctic communities.

Further research in both the indirect and direct consequences of a lengthened open water season would be useful to understand how predicted changes in ice cover will impact the day-to-day lives of Arctic community members.

Some further analysis to the Chapter 2 indices relating to the open water wind events could include more observations from community members in terms of defining what constitutes a true freeze-up and break-up. This would involve interviewing members of each community to be examined, in order to determine a blanketing definition of freeze-up and break-up. Ideally, these definitions would pertain to common activities or transportation routes. Another useful addition to the work done in Chapter 2 which relates to the increases water set-up along the coastline would be to implement observations of water levels as they relate to wind speeds and directions. This could potentially be done by implementation of tide gauges, which are lacking in Alaska (Alaska Department of Natural Resources, 2018).

To expand on the work done here pertaining to the physical mechanisms of freeze-up, it would be useful to extend the analysis so that it uses projected sea ice cover with predicted wind patterns on a seasonal scale (e.g. stormy or calm season). Given the results found in Chapter 3, we can expect regional differences in the projections of sea ice cover. If we were to do a model run for the next 100 years, it would be interesting to evaluate how often this positive correlation holds in the Chukchi Sea and southern Beaufort, and how often the negative correlation is shown in the Bering Sea.

References

Aagaard, K. and Roach, A. (1990). Arctic ocean-shelf exchange: Measurements in barrow canyon. *Journal of Geophysical Research: Oceans*, **95**(C10), 18163–18175.

Alaska Department of Natural Resources (2018). Division of Geological and Geophysical Surveys: Coastal Hazards. http://dggs.alaska.gov/sections/engineering/profiles/coastalhazards.html. Accessed: 2018-06-20.

Asplin, M. G., Galley, R., Barber, D. G., and Prinsenberg, S. (2012). Fracture of summer perennial sea ice by ocean swell as a result of arctic storms. *Journal of Geophysical Research: Oceans*, **117**(C6).

Barnhart, K. R., Anderson, R. S., Overeem, I., Wobus, C., Clow, G. D., and Urban, F. E. (2014). Modeling erosion of ice-rich permafrost bluffs along the alaskan beaufort sea coast. *Journal of Geophysical Research: Earth Surface*, **119**(5), 1155–1179.

Bourke, R. H. and Paquette, R. G. (1976). Atlantic water on the chukchi shelf. *Geophysical Research Letters*, **3**(10), 629–632.

Chukchi Sea Environmental Studies Program (2018). CSESP. https://www.chukchiscience.com/Downloads/. Accessed: 2018-04-19.

Ford, J. D. and Pearce, T. (2010). What we know, do not know, and need to know about climate change vulnerability in the western canadian arctic: a systematic literature review. *Environmental Research Letters*, **5**(1), 014008.

Hauri, C., Winsor, P., Juranek, L. W., McDonnell, A. M., Takahashi, T., and Mathis, J. T. (2013). Wind-driven mixing causes a reduction in the strength of the continental shelf carbon pump in the chukchi sea. *Geophysical Research Letters*, **40**(22), 5932–5936.

Hughes, M. and Cassano, J. J. (2015). The climatological distribution of extreme arctic winds and implications for ocean and sea ice processes. *Journal of Geophysical Research: Atmospheres*, **120**(15), 7358–7377.

Johnson, M. and Eicken, H. (2016). Estimating arctic sea-ice freeze-up and break-up from the satellite record: A comparison of different approaches in the chukchi and beaufort seas. *Elem Sci Anth*, **4**.

Johnston, M., Dawson, J., De Souza, E., and Stewart, E. J. (2017). Management challenges for the fastest growing marine shipping sector in arctic canada: Pleasure crafts. *Polar Record*, **53**(1), 67–78.

Kapsch, M.-L., Eicken, H., and Robards, M. (2010). Sea ice distribution and ice use by indigenous walrus hunters on st. lawrence island, alaska. In *SIKU: Knowing Our Ice*, pages 115–144. Springer.

Mathis, J. T. and Questel, J. M. (2013). Assessing seasonal changes in carbonate parameters across small spatial gradients in the northeastern chukchi sea. *Continental Shelf Research*, **67**, 42–51.